Production and Dispersion Stability of Ultrafine Al, Cu and Al-Cu Particles in Base Fluid for Heat Transfer Applications

**A thesis submitted
in
partial fulfillment of the requirement for the award of degree
of**

**Master of Technology
in
Metallurgical and Materials Engineering**

Submitted

By

Sumanta Samal

Roll No. 207MM107

**Department of Metallurgical and Materials Engineering
National Institute of Technology, Rourkela-769008
May 2009**

Production and Dispersion Stability of Ultrafine Al, Cu and Al-Cu Particles in Base Fluid for Heat Transfer Applications

A thesis submitted

in

partial fulfillment of the requirement for the award of degree

of

Master of Technology

in

Metallurgical and Materials Engineering

Submitted

By

Sumanta Samal

Roll No. 207MM107

Under the Supervision of

Prof. D. Chaira

Department of Metallurgical and Materials Engineering
National Institute of Technology, Rourkela-769008
May 2009

National Institute of Technology
Rourkela

<u>Certificate</u>

This is to certify that the thesis entitled "**Production and Dispersion Stability of Ultrafine Al, Cu and Al-Cu Particles in Base Fluid for Heat Transfer Applications**" submitted by Sri Sumanta Samal in partial fulfillment of the requirements for the award of Master of Technology in Metallurgical and Materials Engineering with specialization in "Metallurgical and Materials Engineering" at National Institute of Technology, Rourkela (Deemed University) is an authentic work carried out by him under my supervision and guidance.

To the best of my knowledge, the matter embodied in the thesis has not been submitted to any other University/Institute for the award of any Degree or Diploma.

Supervisor

Prof. Debasis Chaira

Department of Metallurgical & Material Engineering

National Institute of Technology,

Rourkela- 769008

Acknowledgement

List of Figures

List of Tables

Abstract

Nanofluid is a stable colloidal suspension of low volume fraction of ultrafine solid particles in nanometric dimension dispersed in conventional heat transfer fluid to offer a dramatic enhancement in conductivity. A two step approach of synthesis of Al, Cu & Al-Cu nanoparticles by mechanical alloying and then dispersing them in base fluid to prepare nanofluids has been adopted here.

Elemental Al & Cu powders were milled separately in a high energy planetary mill at a speed of 300 rpm and at 10:1 ball to powder weight ratio. Milling was carried out for 50 hours in wet condition (about 50 ml of toluene) to prevent undue oxidation. In another set of experiment, mixture of elemental Al and Cu (50 atomic wt. %) were milled in planetary mill at the same milling conditions. Powders were picked up from the mill after selected milling time to see the change in size reduction and morphology of powders. Powder particles were characterized by x-ray diffraction (XRD), scanning electron microscopy (SEM), particle size analyzer, and transmission electron microscopy (TEM). It is found from XRD that the crystallite size is around 31 nm for both Al and Cu whereas 6 nm for Al-Cu alloy. The lattice strain value is around 0.37, 0.29 & 1.42 % for Al, Cu & Al-Cu respectively. After 50 hours of milling, particles size has been reduced to 500 nm for Al, 400 nm for Cu and 300 nm for Al-Cu. It is also found from transmission electron microscopy (TEM) that each particles consists of large number of crystallites of size around 10-15 nm.

The milled powders were then dispersed by ultrasonication and magnetic stirring in deionized water to prepare nanofluids. The stability of nanofluids was also studied by nanozeta meter at different pH of nanofluids for constant ultrasonication time and magnetic stirring. It has been found from Nanozeta meter that the suspension is best stable at pH value of 5.5, 9.8 and 9.5 corresponding to zeta potential value of -55.50, -74.55 and -90.60 mV for Al, Cu and Al-Cu respectively with the presence of surfactant.

Contents

Chapter -1

Introduction

1.1 Introduction

Heat transfer is one of the most important processes in many industrial and consumer products. The inherently poor thermal conductivity of conventional fluids puts a fundamental limit on heat transfer. Therefore, for more than a century since Maxwell [1], scientists and engineers have made great efforts to break this fundamental limit by dispersing millimeter- or micrometer-sized particles in liquids. However, the major problem with the use of such large particles is the rapid settling of these particles in fluids, clogging and erosion of pipes and channels. As extended surface technology has already been adapted to its limits in the designs of thermal management systems, technologies with the potential to improve a fluid's thermal properties are of great interest once again. The concept and emergence of nanofluids is related directly to trend in miniaturization and nanotechnology. Maxwell's concept is old, but what is new and innovative in the concept of nanofluids is the idea that particle size is of primary importance in developing stable and highly conductive nanofluids.

Ultrahigh-performance cooling is one of the most vital needs of many industrial technologies. However, inherently low thermal conductivity is a primary limitation in developing energy efficient heat transfer fluids that are required for ultrahigh-performance cooling. Nanofluids are engineered by suspending nanoparticles with average sizes below 100 nm in traditional heat transfer fluids such as water, oil, and ethylene glycol. Nanofluids (nanoparticle fluid suspensions) is the term coined by Choi [2] to describe this new class of nanotechnology-based heat transfer fluids that exhibit thermal properties superior to those of their host fluids or conventional particle fluid suspensions. Nanofluid technology, a new interdisciplinary field of great importance where nanoscience, nanotechnology, and thermal engineering meet, has developed largely over the past decade. The goal of nanofluids is to achieve the highest possible thermal properties at the smallest possible concentrations (preferably<1% by volume) by uniform dispersion and stable suspension of nanoparticles (preferably<10 nm) in base fluids.

Based upon the above discussion of the versatile properties and applications of nanofluids, we have made an approach to synthesize Al, Cu, Al-Cu based nanofluids which can transfer heat more effectively. In the present study, the primary objectives are to synthesize elemental

ultrafine particles Al, Cu and Al-Cu alloy & then preparation of stable dispersion of ultrafine particles in base fluid to develop heat transfer fluids.

1.2 Objectives and Scope of the Present Study

➢ Synthesize ultrafine Al, Cu and Al-Cu alloy particles through mechanical alloying process by 50 hours of planetary ball milling.

➢ Characterize the ultrafine particles by different characterization techniques like XRD, SEM, TEM, and Particle size analyzer.

➢ Preparation of Al, Cu and Al-Cu based Nanofluids by dispersing particles in base fluid with the help of ultrasonic probe and magnetic stirrer.

➢ Study of dispersion stability of Al, Cu and Al-Cu alloy ultrafine particles in base fluid by Nano zeta meter at different pH with and without addition of surfactant.

1.3 Scope of the thesis

The organization of the rest of the thesis is as follows. The development, concept of nanofluids, theoretical study, potential benefit, applications and methods of producing nanofluids are provided in chapter 2. A detailed experimental study and different characterization techniques are provided in chapter 3. This chapter also provides a description of the milling experiments for the synthesis of Al, Cu, Al-Cu ultrafine particles, different characterization techniques and synthesis of Al, Cu, Al-Cu based nanofluids. In chapter 4, characterization of the ultrafine particles synthesized from elemental Al and Cu powder is presented. This chapter also provides the dispersion stability of ultrafine particles in base fluid. A summary of the main findings along with conclusions is presented in chapter 5. Chapter 6 and 7 provides the future work of nanofluid and references respectively.

Chapter -2

Literature Survey

2.1 Literature Background

2.1.1 Development and concept of nanofluids

Since Nobel prize winner Richard P. Feynman presented the concept of micromachines in his seminal talk, "There's Plenty of Room at the Bottom—An Invitation to Enter a New Field of Physics," in December 1959 at the annual meeting of the American Physical Society at the California Institute of Technology, miniaturization has been a major trend in modern science and technology [3]. In 1962, the Japanese thermodynamicist Kubo [4] showed that the electronic level of a fine metallic grain could change according to the difference in the particle size. Gerd Binnig and Heinrich Rohrer of the IBM laboratory in Switzerland developed a new scanning tunneling microscopy (STM) technology in early 1980, developing images of the atomic structure on the surface of objects, which enabled further development for the foundation of nanomaterials. Nobel Prize winner, H. Rohrer, presented the chances and challenges of the "nano-age" [5]. Nano is a prefix meaning one-billionth, so a nanometer is one-billionth of a meter. Nanotechnology is the creation of functional materials, devices, and systems by controlling matter at the nanoscale level, and the exploitation of their novel properties and phenomena that emerge at that scale. The steady miniaturization trend has dropped from the millimeter scale of the early 1950s to the present-day atomic scale [6]. Nanofluid technology will thus be an emerging and exciting technology of the twenty-first century. With the continued miniaturization of technologies in many fields, nanofluids with a capability of cooling high heat fluxes exceeding 1000 W/cm^2 would be paramount in the advancement of all high technology.

Nanofluids have attracted attention as a new generation of heat transfer fluids with superior potential for enhancing the heat transfer performance of conventional fluids. These fluids are obtained by a stable colloidal suspension of low volume fraction of ultrafine solid particles in nanometric dimension dispersed in conventional heat transfer fluid such as water, ethylene glycol or propylene glycol in order to enhance or improve its rheological, mechanical, optical, and thermal properties. The concept of nanofluid was first coined by S.U.S Choi [2] at Argonne National Laboratory and have attracted considerable interest because of reports of great enhancement of heat transfer [7, 2], mass transfer [8], and wetting and spreading [9].It is well known that at room temperature, metals in solid form have orders-of magnitude higher

thermal conductivities than those of fluids [10]. For example, the thermal conductivity of copper at room temperature is about 700 times greater than that of water and about 3000 times greater than that of engine oil, as shown in Table 2.1 and Fig 2.1. The thermal conductivity of metallic liquids is much greater than that of nonmetallic liquids. Therefore, the thermal conductivities of fluids that contain suspended solid metallic particles could be expected to be significantly higher than those of conventional heat transfer fluids.
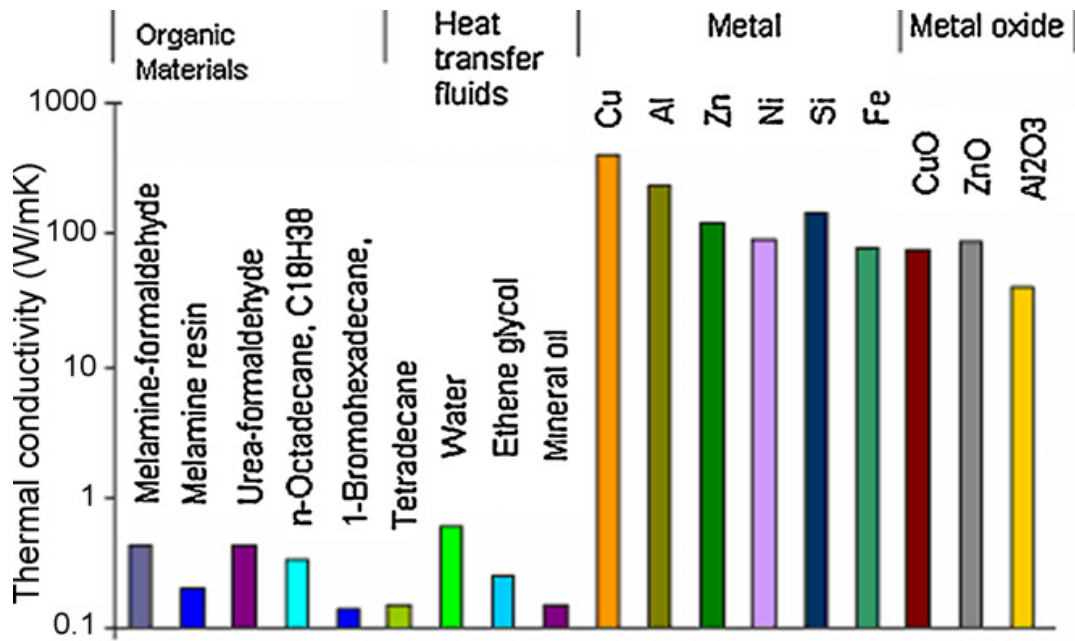
Fig 2.1 Comparison of the thermal conductivity of common liquids, polymers and solids.

Table 2.1 Solids have thermal conductivities that are orders of magnitude larger than those of conventional heat transfer fluids.

	Material	Thermal Conductivity (W/m · K) [a]
Metallic solids	Silver	429
	Copper	401
	Aluminum	237
Nonmetallic solids	Diamond	3300
	Carbon nanotubes	3000
	Silicon	148
	Alumina (Al_2O_3)	40
Metallic liquids	Sodium at 644 K	72.3
Nonmetallic liquids	Water	0.613
	Ethylene glycol	0.253
	Engine oil	0.145

a At 300K unless otherwise noted.

It was found by several researchers that the thermal conductivity of these fluids can be significantly increased when compared to the same fluids without nanoparticles. Since thermal conductivity of solids is orders of magnitude greater than that of liquids, dispersion of solid particles in a given fluid is bound to increase its thermal conductivity.

Fluids are essential for heat transfer in many engineering equipments. Low thermal conductivity of conventional heat transfer fluids such as water, oil, and ethylene glycol mixture is a serious limitation in improving the performance and compactness of these engineering equipments. The dispersion of a low volume (<1%) fraction of solid nanoparticles in traditional base fluid drastically increases the thermal conductivity than that of base fluid [11, 12]. Lee et al. [13] demonstrated a maximum increase in the thermal conductivity of approximately 20% when CuO nanoparticles were suspended in ethylene glycol. Suspending copper nanoparticles, average diameter size less than 10 nm, Eastman et

al. [14] were able to increase thermal conductivity of ethylene glycol up to 40%. In the same year, Choi et al. [15] were able to report 160% increase of a synthetic poly oil thermal conductivity when metallic multi-wall nanotubes were suspended. Das et al. [16] observed that the thermal conductivity for nanofluid increases with increasing temperature. A small amount (<1% volume fraction) of Cu nanoparticles or carbon nanotubes dispersed in water or oil was reported to increase the inherently poor thermal conductivity of the liquid by 74% and 150% [17, 15]. Furthermore, the 300% enhancement of thermal conductivity observed by Philip was achieved by a Fe_3O_4 nanoparticle loading of 6.3 vol. % [18].

The enhancement of thermal conductivity of nanofluid over conventional base fluid like de-ionized water; ethylene glycol etc. has several applications starting from closely packed integrated circuits at small scale industry to nuclear reactor at large scale. The thermal conductivity of these fluids plays a vital role in the development of energy-efficient heat transfer equipment.

However, dispersion of milli- and micrometer-sized particles is prone to sedimentation, clogging and erosion of pipes and channels. Compared to conventional solid-liquid suspensions for heat transfer intensifications, properly engineered thermal nanofluids possess the following advantages:

i) High specific surface area and therefore more heat transfer surface between particles and fluids.
ii) High dispersion stability with predominant Brownian motion of particles.
iii) Reduced pumping power as compared to pure liquid to achieve equivalent heat transfer intensification.
iv) Reduced particle clogging as compared to convention slurries, thus promoting system miniaturization.
v) Adjustable properties, including thermal conductivity and surface wettability, by varying particle concentrations to suit different applications.

The nanofluid is stable [19], introduce very little pressure drop and it can pass through nano-channels. The stability of suspension is one of the crucial factors required for improving the thermal conductivity of the fluid and its applications as an efficient coolant [20]. The stability

6

can be increased by adding suitable third agent like oleic acid, laurate salt or a fatty acid [21, 16].

Several approaches have been used to disperse the particles

i) Changing the pH value of suspension;

ii) Using surface activator and dispersants, few dispersants ammonium citrate (aqueous) and imidazoline or oleyl alcohol (nonaqueous) are promising additives for deagglomeration;

iii) Using ultrasonic vibration.

These techniques can change the surface properties of the particles. Some commercially available prepared nanofluids have been found to contain unacceptable levels of impurities. The presence of dispersants and chemical reagents could influence the physical, thermal, and chemical properties of the nanofluids.

2.1.2 Theoretical studies on nanofluids

2.1.2.1 Underlying mechanisms for the enhanced thermal conductivity of nanofluids

The classical models [1, 22] which were developed from the effective medium theory for the effective thermal conductivity of composites have been verified by experimental data for mixtures with low concentrations of milli- or micrometer- sized particles. Experiments have shown that nanofluids exhibit anomalously high thermal conductivity, which cannot be predicted accurately by the classical models. To explain the observed enhanced thermal conductivity of nanofluids, Wang et al. [23] and Keblinski et al. [24] proposed various mechanisms, which were not considered by classical models.

Wang et al. [23] suggested that the microscopic motion of nanoparticles, the surface properties, and the structural effects might cause enhanced thermal conductivity of nanofluids. In nanofluids, the microscopic motion of the nanoparticles due to Brownian motion, van der Waals force, and electrostatic force can be significant. Wang et al. however, showed that Brownian motion does not contribute significantly to the heat energy transport in nanofluids. They indicated that the electric double layer and van der Waals force could have strong electrokinetic effects on the nanoparticles. The surface properties and structural effects were not confirmed as potential mechanisms in their study.

Keblinski et al. [24] later elucidated four possible mechanisms for the anomalous increase in nanofluids heat transfer, and these mechanisms are

i) Brownian motion of the nanoparticles,

ii) Liquid layering at the liquid/particle interface,

iii) Nature of the heat transport in the nanoparticles,

iv) The effect of nanoparticle clustering.

i) Brownian motion of the nanoparticles

Brownian motion is caused by the random bombardment of liquid molecules. Due to the Brownian motion, particles randomly move through the liquid, thereby enabling stronger transport of heat (compared to sole heat conduction), which can increase the effective thermal conductivity. For Brownian motion to be a significant contributor to the thermal conductivity, it would have to be a more efficient mechanism than thermal diffusion in the fluid.

ii) Liquid layering at the liquid/particle interface

Liquid layering around the particle (i.e. nanolayer) was proposed as another responsible mechanism accounting for higher thermal properties of nanofluids. The basic idea is that liquid molecules can form a layer around the solid particles and thereby enhance the local ordering of the atomic structure at the interface region. Hence, the atomic structure of such liquid layer is significantly more ordered than that of the bulk liquid. Given that solids, which have much ordered atomic structure, exhibit much higher thermal conductivity than liquids, the liquid layer at the interface would reasonably have a higher thermal conductivity than the bulk liquid. Thus the nanolayer is considered as an important factor enhancing the thermal conductivity of nanofluids.

iii) Nature of the heat transport in the nanoparticles

When the size of the nanoparticles in a nanofluid becomes less than the phonon mean-free path, phonons no longer diffuse across the nanoparticle but move ballistically without any scattering. However, it is difficult to envision how ballistic phonon transport could be more effective than a very-fast diffusion phonon transport, particularly to the extent of explaining anomalously high thermal conductivity of nanofluids.

iv)The effect of nanoparticle clustering

The effective volume of a cluster is considered much larger than the volume of the particles due to the lower packing fraction (ratio of the volume of the solid particles in the cluster to the total volume of the cluster) of the cluster. Since heat can be transferred rapidly within such clusters, the volume fraction of the highly conductive phase (cluster) is larger than the volume of solid, thus increasing its thermal conductivity. It is however noted that in general, clustering may also exert a negative effect on heat transfer enhancement, particularly at a low volume fraction by settling small particles out of the liquid and creating a large regions of ''particle free'' liquid with a high thermal resistance. Besides these mechanisms, it is the authors' believe that the effects of particle surface chemistry and particles interaction for nanometer-sized particles could be significant in enhancing the thermal conductivity of nanofluids.

2.1.2.2 Electrokinetic phenomena of nanofluids

Electrochemical effects certainly influence the thermal conductivity of nanofluids through stability and particle interactions. For example, the electrostatic repulsive force, which is described by the zeta potential, is important to avoiding agglomeration and thus sedimentation of nanoparticles. Patel et al. [25] reported that 4 nm gold nanoparticles with a coating of a covalent chain in toluene were about 50 times less effective for heat transport than uncoated 10–20 nm gold particles in water. Lee et al. [26] investigated the effect of zeta potential and particle hydrodynamic size (i.e. the mobility equivalent size) on the thermal conductivity of nanofluids. The hydrodynamic diameter of CuO nanoparticles and thermal conductivity of the nanofluids at different pH values were measured in their study. Their results demonstrated that the pH value affects the thermal performance of the nanofluids. As the solution pH value departs from the iso-electric point of particles, the colloidal particles become more stable and eventually alter the thermal conductivity of the fluid. They identified that the surface charge state is primarily responsible for the enhancement of thermal conductivity of the nanofluids.

2.1.2.3 Convective heat transfer studies of nanofluids

Compared to the reported research on thermal conductivity, investigations on convective heat transfer of nanofluids are scarce. A summary of previous studies on forced convection heat transfer of nanofluids [27] is given in Table 2.2.

Table 2.2 Summary of forced convection heat transfer experimental studies of nanofluids.

Researchers	Geometry/flow nature	Nanofluids	Findings
Pak and Cho [28]	Tube/turbulent	Al_2O_3 (13 nm), TiO_2 (27 nm)/water	At 3 vol.%, the convective heat transfer coefficient (h) was 12% smaller than pure water for a given average fluid velocity
Xuan and Li [29]	Tube/turbulent	Cu (<100 nm)/water	A larger enhancement of h with volume fraction (ϕ) and Reynolds number (Re) was observed
Wen and Ding [30]	Tube/laminar	Al_2O_3 (13 nm)/water	Increased h with ϕ and Reynolds number was observed
Ding et al. [31]	Tube/laminar	CNT/water	At 0.5 wt.%, h increased by more than 350 % at Re = 800
Heris et al. [32]	Circular tube/laminar	Al_2O_3 (20 nm), CuO (50–60 nm)/water	h increase with ϕ and Pe. Al_2O_3 shows higher enhancement than that of CuO
Lai et al. [33]	Tube/laminar	Al_2O_3 (20 nm)/DIW	Nu increased 8% for ϕ=0.01 and Re = 270
Jung et al. [34]	Rectangular microchannel/laminar	Al_2O_3 (20 nm)/water	h increased 15% for ϕ = 0.018

Pak and Cho performed experiments on convective heat transfer of two types of nanofluids i.e. γ Al_2O_3 and TiO_2 dispersed in water, under turbulent flow conditions. Even though the Nusselt number (Nu) was found to increase with the particle volume fraction and the Reynolds number, the heat transfer coefficient (h) actually decreased by 3–12%.

The experimental results of Xuan and Li illustrated that the convective heat transfer coefficient of Cu/water based nanofluids varied significantly with the flow velocity and the volumetric loading of particles. For example, for 2 vol% of Cu nanoparticles in water, the Nusselt number increased by about 60%.

Wen and Ding presented the convective heat transfer characteristics of nanofluids at the tube entrance region under laminar flow conditions. The experiments were conducted for 600 < Re < 2200. Their results illustrate that the local heat transfer coefficient varies with ϕ and Re. For example, for $\phi = 0.016$ and at x/D = 63, the local h was 41% higher for Re = 1050, and 47% higher for Re = 1600, compared with the results for pure water. The enhancement was particularly significant in the entrance region and decreased with axial distance.

The same research group later conducted convective heat transfer experiments for CNT-based nanofluids in laminar flow and constant wall heat flux conditions. Surprisingly, the maximum increase in the convective heat transfer coefficient was more than 350% at Re = 800 and at 0.5 weight % of CNT.

Heris et al. investigated convective heat transfer of CuO and Al_2O_3/water-based nanofluids under laminar flow conditions through an annular copper tube. In their study, the heat transfer coefficient was found to increase with increasing particle volume fraction as well as Peclet number. Al_2O_3/water-based nanofluids showed higher enhancement of heat transfer coefficient compared to CuO/water-based nanofluids.

Lai et al. studied Al_2O_3 (20 nm)/DIW-based nanofluids flowing through 1 mm sized stainless steel test tube and subjected to constant wall heat flux and low Reynolds number (Re < 270). Compared to the base fluid, the Nusselt number of this nanofluid had a maximum enhancement of 8% for 1 vol% nanoparticle at Re = 270.

Jung et al. conducted convective heat transfer experiments for Al_2O_3/water-based nanofluid in a rectangular microchannel (50x50 $micron^2$) under laminar flow conditions. The convective heat transfer coefficient increased by more than 32% for 1.8 vol% of nanoparticles in base fluids. The Nusselt number increases with increasing Reynolds number in the laminar flow regime (5 < Re < 300). Based on the results, they proposed a new convective heat transfer correlation for nanofluids in microchannels. The above review shows that the results reported by various groups vary widely and most of the studies lack physical explanation for their observed results. Therefore, further research on convective heat transfer of nanofluids is needed.

2.1.3 Impact and potential benefits of nanofluids

The impact of nanofluid technology is expected to be great considering that heat transfer performance of heat exchangers or cooling devices is vital in numerous industries. For example, the transport industry has a need to reduce the size and weight of vehicle thermal management systems and nanofluids can increase thermal transport of coolants and lubricants. When the nanoparticles are properly dispersed, nanofluids can offer numerous benefits [35-37] besides the anomalously high effective thermal conductivity. These benefits include:

2.1.3.1 Improved heat transfer and stability: Because heat transfer takes place at the surface of the particles, it is desirable to use particles with larger surface area. The relatively larger surface areas of nanoparticles compared to microparticles, provide significantly improved heat transfer capabilities. In addition, particles finer than 20 nm carry 20% of their atoms on their surface, making them instantaneously available for thermal interaction [36]. With such ultra-fine particles, nanofluids can flow smoothly in the tiniest of channels such as mini- or micro-channels. Because the nanoparticles are small, gravity becomes less important and thus chances of sedimentation are also less, making nanofluids more stable.

2.1.3.2 Microchannel cooling without clogging: Nanofluids will not only be a better medium for heat transfer in general, but they will also be ideal for microchannel applications where high heat loads are encountered. The combination of microchannels and nanofluids will provide both highly conducting fluids and a large heat transfer area. This cannot be attained with macro- or micro-particles because they clog microchannels.

2.1.3.3 Miniaturized systems: Nanofluid technology will support the current industrial trend toward component and system miniaturization by enabling the design of smaller and lighter heat exchanger systems. Miniaturized systems will reduce the inventory of heat transfer fluid and will result in cost savings.

2.1.3.4 Reduction in pumping power: To increase the heat transfer of conventional fluids by a factor of two, the pumping power must usually be increased by a factor of 10. It was

shown that by multiplying the thermal conductivity by a factor of three, the heat transfer in the same apparatus was doubled [2]. The required increase in the pumping power will be very moderate unless there is a sharp increase in fluid viscosity. Thus, very large savings in pumping power can be achieved if a large thermal conductivity increase can be achieved with a small volume fraction of nanoparticles.

2.1.3.5 Cost and Energy Savings: Successful employment of nanofluids will result in significant energy and cost savings because heat exchange systems can be made smaller and lighter.

The better stability of nanofluids will prevent rapid settling and reduce clogging in the walls of heat transfer devices. The high thermal conductivity of nanofluids translates into higher energy efficiency, better performance, and lower operating costs. They can reduce energy consumption for pumping heat transfer fluids. Miniaturized systems require smaller inventories of fluids where nanofluids can be used. Thermal systems can be smaller and lighter. In vehicles, smaller components result in better gasoline mileage, fuel savings, lower emissions, and a cleaner environment [38].

2.1.4 Potential applications of nanofluids

The heat transport is very important for nanotechnology applications [39]. In general way is important to learn about how to manipulate and control the heat transport at nanoscale dimensions, which without doubt, will open ways to improve new applications. With the aforementioned highly desired thermal properties and potential benefits, nanofluids can be seen to have a wide range of industrial and medical applications, which are elaborated here.

2.1.4.1 Engineering applications

Nanofluids can be used to improve thermal management systems in many engineering applications including:

(a) Nanofluids in transportation

The transportation industry has a strong demand to improve performance of vehicle heat transfer fluids and enhancement in cooling technologies is also desired. Because engine coolants, engine oils, automatic transmission fluids, and other synthetic high temperature

fluids currently possess inherently poor heat transfer capabilities, they could benefit from the high thermal conductivity offered by nanofluids. Nanofluids would allow for smaller, lighter engines, pumps, radiators, and other components. Lighter vehicles could travel further on the same amount of fuel i.e. more mileage per liter. More energy-efficient vehicles would save money. Moreover, burning less fuel would result in lower emissions and thus reduce environment pollution. Therefore, in transportation systems, nanofluids can contribute greatly. An ethylene glycol and water mixture, the nearly universally used automotive coolant, is a relatively poor heat transfer fluid compared to water alone. Engine oils perform even worse as a heat transfer medium. The addition of nanoparticles to the standard engine coolant has the potential to improve automotive and heavy-duty engine cooling rates. Such improvement can be used to remove engine heat with a reduced-size coolant system. Smaller coolant systems result in smaller and lighter radiators, which in turn benefit almost every aspect of car and truck performance and lead to increased fuel economy. Alternatively, improved cooling rates for automotive and truck engines can be used to remove more heat from higher horsepower engines with the same size of coolant system. A promising nanofluid engine coolant is pure ethylene glycol with nanoparticles. Pure ethylene glycol is a poor heat transfer fluid compared to a 50/50 mixture of ethylene glycol and water, but the addition of nanoparticles will improve the situation. If the resulting heat transfer rate can approach the 50/50 mixture rate, there are important advantages. Perhaps one of the most prominent is the low-pressure operation of an ethylene-glycol-based nanofluid compared with a 50/50 mixture of ethylene glycol and water. An atmospheric-pressure coolant system has lower potential capital cost. This nanofluid also has a high boiling point, which is desirable for maintaining single-phase coolant flow. In addition, a higher boiling point coolant can be used to increase the normal coolant operating temperature and then reject more heat through the existing coolant system. More heat rejection allows a variety of design enhancements, including engines with higher horsepower.

(b) In micromechanics and instrumentation

Since 1960s, miniaturization has been a major trend in science and technology. Microelectromechanical systems (MEMS) generate a lot of heat during operation. Conventional coolants do not work well with high power MEMS because they do not

have enough cooling capability. Moreover, even if large-sized solid particles were added to these coolants to enhance their thermal conductivity, they still could not be applied in practical cooling systems, because the particles would be too big to flow smoothly in the extremely narrow cooling channels required by MEMS. Since nanofluids can flow in microchannels without clogging, they would be suitable coolants. They could enhance cooling of MEMS under extreme heat flux conditions.

(c) In heating, ventilating and air-conditioning (HVAC) systems

Nanofluids have potential application in building where increases in energy efficiency could be realized without increased pumping power. Such an application would save energy in a heating, ventilating, and air conditioning system while providing environmental benefits. Nanofluids could improve heat transfer capabilities of current industrial HVAC and refrigeration systems. Many innovative concepts are being considered; one involves pumping of coolant from one location where the refrigeration unit is housed in another location. Nanofluid technology could make the process more energy efficient and cost effective.

(d) Electronics Cooling

The power density of integrated circuits and microprocessors has increased dramatically in recent years. The trend should continue for the foreseeable future. Recently, the International Technology Roadmap for Semiconductors (ITRS) projected that, by 2018, high-performance integrated circuits will contain more than 9.8 billion transistors on a chip area of 280 mm^2 - more than 40 times as many as today's chips of 90-nm node size. Future processors for high-performance computers and servers have been projected to dissipate higher power, in the range of 100-300 W/cm^2. Whether these values actually become reality is not as significant as the projection that the general trend to higher power density electronics will continue. Existing air-cooling techniques for removing this heat are already reaching their limits, and liquid cooling technologies are being, and have been, developed for replacing them. Single-phase fluids, two-phase fluids, and nanofluids are candidate replacements for air. All have increased heat transfer capabilities over air systems, and all are being investigated.

(e) Space and Defense

A number of military devices and systems require high-heat-flux cooling to the level of tens of MW/m^2. At this level, cooling with conventional fluids is challenging. Examples of military applications include cooling of power electronics and directed-energy weapons. Directed-energy weapons involve high heat fluxes (> 500 - 1000 W/cm^2), and providing adequate cooling of them and the associated power electronics is a critical need. Nanofluids have the potential to provide the required cooling in such applications as well as in other military systems, including military vehicles, submarines, and high-power laser diodes. In some cases, nanofluid research for defense applications includes multifunctional nanofluids with added thermal energy storage or energy harvesting through chemical reactions. Transformer cooling is important to the Navy as well as the power generation industry with the objective of reducing transformer size and weight. The ever-growing demand for greater electricity production can lead to the necessity of replacing and/or upgrading transformers on a large scale and at a high cost. A potential alternative in many cases is the replacement of conventional transformer oil with a nanofluid. Such retrofits can represent considerable cost savings. It has been demonstrated that the heat transfer properties of transformer oils can be significantly improved by using nanoparticle additives.

Recent experiments have shown some promising nanofluids with amazing properties such as fluids with advanced heat transfer, drag reduction, binders for sand consolidation, gels, products for wettability alteration, and anticorrosive coatings [9, 40].

A great deal of energy is expended heating industrial and residential buildings in the cold regions of the world. Due to the severe winter conditions, ethylene glycol or propylene glycol mixed with water in different volume percentages are typically used to lower the aqueous freezing point of the heat transfer medium [41]. Such heat transfer fluids are used in baseboard heaters in homes, heat exchangers, automobiles and in industrial plants in cold regions. These fluids can withstand very low temperatures. At low temperatures, ethylene glycol mixtures have better heat transfer characteristics than propylene glycol mixtures [42]. In the renewable energy industry, nanofluids could be employed to enhance heat transfer from solar collectors to storage tanks and to increase the energy

density. Nanofluid coolants also have potential application in major process industries, such as materials, chemical, food and drink, oil and gas, paper and printing, and textiles.

2.1.4.2 Medical applications

Nanofluids and nanoparticles have many applications in the biomedical industry. For example, to circumvent some side effects of traditional cancer treatment methods, iron-based nanoparticles could be used as delivery vehicles for drugs or radiation without damaging nearby healthy tissue. Such particles could be guided in the bloodstream to a tumor using magnets external to the body. Nanofluids could also be used for safer surgery by producing effective cooling around the surgical region and thereby enhancing the patient's chance of survival and reducing the risk of organ damage. In a contrasting application to cooling, nanofluids could be used to produce a higher temperature around tumors to kill cancerous cells without affecting nearby healthy cells. Magnetic nanoparticles in body fluids (biofluids) can be used as delivery vehicles for drugs or radiation, providing new cancer treatment techniques. Due to their surface properties, nanoparticles are more adhesive to tumor cells than normal cells. Thus, magnetic nanoparticles excited by an AC magnetic field are promising for cancer therapy. The combined effect of radiation and hyperthermia is due to the heat-induced malfunction of the repair process right after radiation-induced DNA damage. Therefore, in future nanofluids can be used as advanced drug delivery fluids. During critical surgery, nanofluids could be used to cool the brain so it requires less oxygen and thereby enhance the patient's chance of survival and reduce the risk of brain damage.

2.1.5 Characteristic Features of Nanofluids

Pioneering nanofluids research in ANL has inspired physicists, chemists, and engineers around the world. Promising discoveries and potentials in the emerging field of nanofluids have been reported.

Nanofluids have an unprecedented combination of the four characteristic features desired in energy systems (fluid and thermal systems):

    i)   Increased thermal conductivity (TC) at low particle concentrations

ii) Strong temperature-dependent TC

iii) Non-linear increase in TC with nanoparticle concentration

iv) Strongly size dependent TC

v) Increase in boiling critical heat flux (CHF)

vi) Increase in the Laminar Heat Transfer Coefficient

vii) Significant increase in the Turbulent Heat Transfer Coefficient

viii) Decrease in the Natural Convection Heat Transfer Coefficient

These characteristic features of nanofluids make them suitable for the next generation of flow and heat-transfer fluids.

2.1.6 Synthesis of nanofluids

Materials for Nanoparticles and Fluids:

Modern fabrication technology provides great opportunities to process materials actively at nanometer scales. Nanostructured or nanophase materials are made of nanometer-sized substances engineered on the atomic or molecular scale to produce either new or enhanced physical properties not exhibited by conventional bulk solids. All physical mechanisms have a critical length scale below which the physical properties of materials are changed. Therefore, particles smaller than 100 nm exhibit properties different from those of conventional solids. The

noble properties of nanophase materials come from the relatively high surface area/volume ratio, which is due to the high proportion of constituent atoms residing at the grain boundaries. The thermal, mechanical, optical, magnetic, and electrical properties of nanophase materials are superior to those of conventional materials with coarse grain structures. Consequently, research and development investigation of nanophase materials has drawn considerable attention from both material scientists and engineers.

1. **Nanoparticle material types**

   Nanoparticles used in nanofluids have been made of various materials, such as oxide ceramics (Al_2O_3, CuO), nitride ceramics (AlN, SiN), carbide ceramics (SiC, TiC), metals (Cu, Ag, Au), semiconductors (TiO_2, SiC), carbon nanotubes, and composite

materials such as alloyed nanoparticles $Al_{70}Cu_{30}$ or nanoparticle core–polymer shell composites In addition to nonmetallic, metallic, and other materials for nanoparticles, completely new materials and structures, such as materials "doped" with molecules in their solid–liquid interface structure, may also have desirable characteristics.

2. **Base liquid types**

   Many types of liquids, such as water, ethylene glycol, oil, acetone, decene have been used as host liquids in nanofluids.

Preparation of nanofluids is the first key step to investigate the heat transfer performance of nanofluids. A nanofluid does not mean a simple mixture of liquid and solid nanoparticles. Techniques for good dispersions of nanoparticles in liquids or directly producing stable nanofluids are crucial. Nanofluids are produced by dispersing nanometer- sized solid particles into liquids such as water, ethylene glycol, or oils. There are mainly two techniques for synthesizing nanofluids, which are

i) **The direct evaporation technique or single-step process** which simultaneously makes and disperses the nanoparticles directly into the base fluids [2, 43-49].
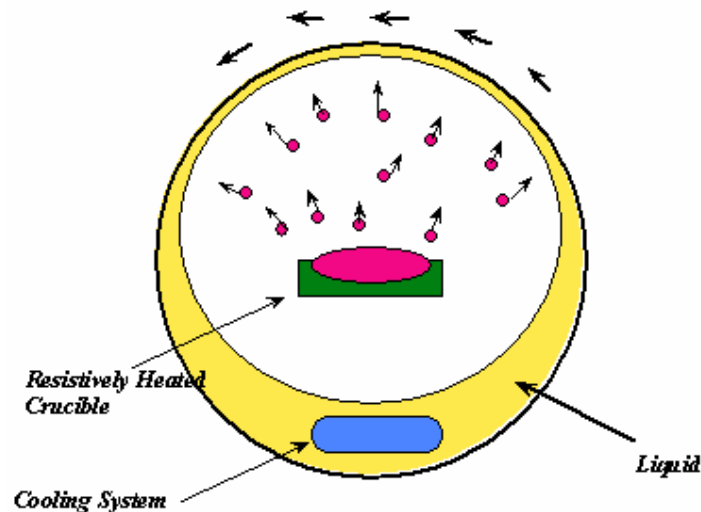

Fig 2.2 Schematic diagram of nanofluid production system designed for direct evaporation of nanocrystalline particles into low-vapor-pressure liquid.

This technique involves the vaporization of a source material under vacuum conditions. An advantage of this process is that nanoparticles agglomeration is minimized. The disadvantages are that the liquid must have a very low vapor pressure and that this technique can produce very limited amounts of nanofluids.

ii) **The two-step method** which represents the formation of nanoparticles and subsequent dispersion of the nanoparticles in the base fluid [11, 12]. Many other routes are used for production of ultrapure nanoparticles like physical and chemical vapour deposition [50],co-precipitation [51–55], sonochemical technique [56-58], sol–gel [59], hydrothermal [60, 61], solution phase method [62–65], electrochemical synthesis [66-69], laser ablation [70, 71].

In the present investigation, the ultrafine particles were prepared by mechanical alloying (MA) with the help of a Fritsch pulverisette-5 planetary ball mill. High energy ball induces high energy impact on the charged powder by collision between balls and powder causing severe plastic deformation, repeated fracturing and cold welding of charged powder leading to the formation of nanoparticles [72-74]. The prepared nanoparticles were dispersed in de-ionized water by ultrasonic probe and magnetic stirrer to prepare desired nanofluid. For nanofluids prepared by the two-step method, dispersion techniques such as high shear and ultrasound can be used to create various particle/fluid combinations.

In either of the case, the production of a uniformly dispersed nanofluid is very necessary for obtaining stable and superior properties of nanofluids [25, 15].

At present, most researchers use the two-step process to produce nanofluids by dispersing commercial or self-produced nanoparticles in a liquid. The optimization (i.e. improvement) of thermal properties of nanofluids requires stable nanofluids, which can be ensured by proper synthesis and dispersion procedures.

Although many experimental studies on nanofluid systems have been performed, the preparation methods for stable nanofluid were not systematically studied yet. In earlier study, stability of carbon black and silver based nanofluid was studied by Soo H. Kim et al. [75]. H. Chang et al. [46] studied the suspension stability of Al_2O_3 nanofluid with different pH. C. Kim et al. [76] studied the effect of sonication on zeta potential value of CuO particles. In the

present study, the primary objectives are to synthesize elemental ultrafine particles Al, Cu and Al-Cu alloy & then preparation of stable dispersion of particles in nanofluid to develop heat transfer fluids.

2.2 Summary

This chapter provides development and concept of nanofluids. This also contains some theoretical study, potential benefit and different applications of nanofluids. Two methods of producing nanofluids i.e. one step process and two step process are described in this chapter.

Chapter – 3

Experimental

3.1 Experimental

3.1.1 Synthesis of ultra fine Al, Cu and Al-Cu particles

Milling was carried out in Pulverisette-5 planetary ball mill with steel vials and steel balls to prepare ultrafine particles. Starting materials used for milling were elemental Al & Cu powder with 99% purity for the synthesis of ultrafine Al and Cu particles. Powder particles were milled for 50h in two vials- each containing 35g powder and 350g steel balls. In another set of experiment, 50 atomic wt % of Cu and Al powders were mixed and milled for 50 hours to prepare ultrafine Al-Cu powder. The ball to powder weight ratio (BPR) was 10:1. Milling was conducted at 300 rpm in wet medium (about 50 ml of toluene) to prevent undue oxidation and agglomeration of powder. Steel balls of diameter 10 mm were used for milling. The specifications for the milling systems are given in Table 3.1.

Table 3.1 The specifications for the milling systems.

Mill type	Fritsch planetary mill
Milling time:	50 hours
Wet milling	media toluene
Milling speed	300 rpm
Grinding media:	
Type	Steel
Ball size	9.3 mm (dia.)
Ball weight/jar	350 g
Ball to powder ratio by weight	10
Jar dimensions	
Length	95 mm
Diameter	75 mm
Jar speed	300rpm

Powder samples were picked up from the vials after selected interval of milling time to see the change in shape and size reduction of powder samples. Powders were characterized by x-ray diffraction (XRD), scanning electron microscopy (SEM), transmission electron microscopy (TEM) and particle size analyzer.

3.1.2 Dispersion of ultrafine particles in base fluid

A very small amount of milled powders (approximately 0.04g) were dispersed in de-ionized water (150 ml) by ultrasonication and subsequently magnetic stirring for about 30 minute each to prepare the desired nanofluid. The test conditions and the specification of materials used for producing desired nanofluids are shown in Table 3.2 and Table 3.3 respectively. The pH was controlled by using acetic acid and ammonium hydroxide. The prepared nanofluids were analyzed by Nano zeta meter to determine the particle size and zeta potential to study the stability of nanofluids at a particular pH.

Table 3.2 The methods of producing nanofluids.

Two-step method of producing nanofluids	Test conditions
Magnetic Stirrer	Revolution speed: 1500 rpm
	Revolution time: 30 min
Ultrasonic disruptor	Sonication time: 30 min
	Frequency: 20 kHz
	Maximum sonicating power: 350 W

Table 3.3 The specification of three materials used for producing nanofluids.

Nanofluid		
Al-water	Cu-water	Al-Cu-water
Particles: Al(Aluminum)	Particles: Cu(Copper)	Particles: Al-Cu
Crystallite size: 31 nm	Crystallite size: 31 nm	Crystallite size: 6 nm
Weight percentage: 0.04 g	Weight percentage: 0.04 g	Weight percentage: 0.04 g
Base fluid: DI-water	Base fluid: DI-water	Base fluid: DI-water
Viscosity: 0.87 mm^2/s	Viscosity: 0.87 mm^2/s	Viscosity: 0.87 mm^2/s
Surfactant: Oleic acid	Surfactant: Oleic acid	Surfactant: oleic acid

Table 3.3 shows the specification of three materials used for producing nanofluids. First, aluminum (Al) ultrafine particles were dispersed in deionized (DI) water with initial concentration of 0.04 g. The crystallite size of Al ultrafine particles was 31 nm. Second, Cu ultrafine particles were mixed with deionized (DI) water with the initial concentration of 0.04 g and the crystallite size of Cu nanoparticles was 31 nm. Third, Al-Cu ultrafine particles were

mixed with deionized (DI) water with the initial concentration of 0.04 g and the crystallite size of cu ultrafine particles was 6 nm. To prevent agglomeration between primary ultrafine particles in the base fluid, oleic acid was added as the surfactants to coat the surface of Al, Cu and Al-Cu nanoparticles, respectively.

3.2 Characterization techniques used

3.2.1 X-Ray Diffraction (XRD) analysis

As a non-destructive testing technique, x-ray diffraction is a powerful tool for the analysis of crystalline structure. X-ray has wavelengths comparable to the crystalline lattice constants, thus it can be used for the accurate measurement of lattice parameter, crystallite size, lattice strain etc.

X-ray diffraction of the as milled powder samples were performed using the diffractometer. X-ray diffraction patterns were recorded from 30° to 110° with a PANalytical system diffractometer (Model: DY-1656) using Cu K_α (λ=1.542A^o) with an accelerating voltage of 40 KV. Data were collected with a counting rate of 3°/min. The K_α doublets were well resolved.

Figure 3.1 PANalytical system diffractometer (Model: DY-1656).

3.2.2 Scanning electron microscopy (SEM) study

The SEM micrographs of as received powder, milled powder samples were obtained using the scanning electron microscope. The images were taken in both secondary electron (SE) and back scattered electron (BSE) mode according to requirement. Microscopic studies to examine the morphology, particle size and microstructure were done by a JEOL 6480 LV scanning electron microscope (SEM) equipped with an energy dispersive X-ray (EDX) detector of Oxford data reference system. Micrographs are taken at suitable accelerating voltages for the best possible resolution using the secondary electron imaging.

Figure 3.2 JEOL JSM-6480LV scanning electron microscope.

3.2.3 Transmission electron microscopy (TEM) study

The instrument used for our TEM analysis was FEI QUANTA model. The TEM micrographs of the milled powder were obtained to determine the true size of the particles. The operating voltage was 200 KV. The samples of TEM have been prepared by mixing the powder with a small amount of pure acetone and stirring for 15 minutes. Two or three drops of the

suspension were placed on carbon coated Cu grid and then well dried for 10 minutes before mounting the grid onto the TEM sample holder.

Figure 3.3 FEI QUANTA transmission electron microscope.

3.2.4 Particle size analysis

Particle size of the milled powder was measured by Malvern particle size analyzer (Model Micro-P, range 0.05-550 micron). Firstly, the liquid dispersant containing 500 ml 0f distilled water and 25 ml of sodium hexa metaphosphate was kept in the sample holder. Then the instrument was run keeping ultrasonic displacement at 10.00 micron and pump speed 1800 rpm. A pinch of powders was added to the liquid dispersant so that the obscuration value varies between 10 to 30% and the residual below 1%.

Figure 3.4 Malvern particle size analyzer (Model Micro-P, range 0.05-550 micron).

3.2.5 Nano zeta sizer

The particle size in nanometer range and dispersion stability of ultrafine particles in nanofluids was measured by Nano zeta sizer (Model: Nano ZS, Malvern). The sample was prepared by dispersing small amount of ultrafine particles in deionized water with constant ultrasonication and magnetic stirring for 30 minutes each. Then the sample was kept in a sample holder with the help of syringe and analyzed.

Figure 3.5 Nano zeta sizer (Model: Nano ZS, Malvern instrument).

3.3 Summary

This chapter contains detailed milling experiments for synthesizing ultra fine Al, Cu and Al-Cu particles and dispersion of ultrafine particles in base fluid with the help of magnetic stirrer and ultrasonic probe. This chapter also provides a description of the milling experiments for the synthesis of Al, Cu, Al-Cu ultrafine particles. Different experimental techniques like X-ray diffraction (XRD), particle size analyzer, scanning electron microscopy (SEM), transmission electron microscopy (TEM), and nano zeta sizer are also provided in this chapter.

Chapter – 4

Results & Discussion

4.1 Results and Discussion

4.1.1 Characterization of Al, Cu and Al-Cu ultrafine particles

4.1.1.1 X-Ray Diffraction (XRD) analysis

The XRD patterns of elemental metallic powder particles at different intervals of milling time are shown in Fig 4.1 and Fig 4.2. It is evident from the figure that the Bragg peaks for milled product (after 50h of milling) are broad, suggesting accumulation of lattice strain and reduction in crystallite size. It is also observed that intensity of the peaks decreases due to the decrease of crystallinity of powder during milling.

In case of Al-Cu alloy powder, the XRD pattern of as received powder shows the peaks of Cu and Al. The final milling product is a single phase nanocrystalline material which is clear from the graph. It is evident from the figure that after 10 hours of milling, Al-Cu has started to form. The figure 4.3 shows that the Bragg peaks for milled product (after 50h of milling) are broad, which shows that lattice strain is accumulated and crystallite size is reduced.
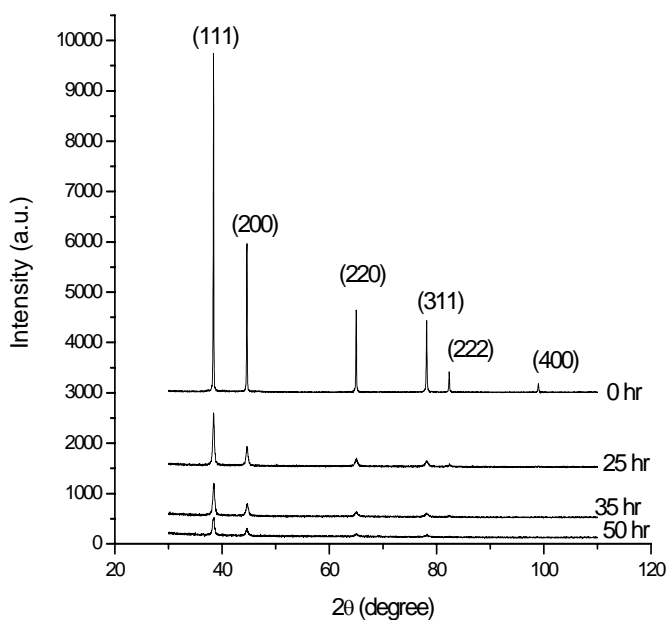
Fig 4.1 XRD patterns of milled powder at selected milling time: Al.
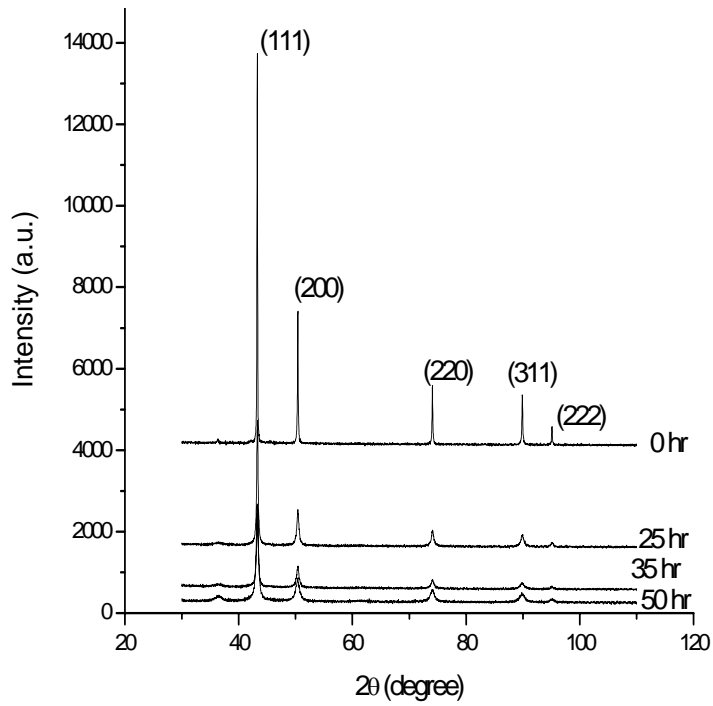
Fig 4.2 XRD patterns of milled powder at selected milling time: Cu.
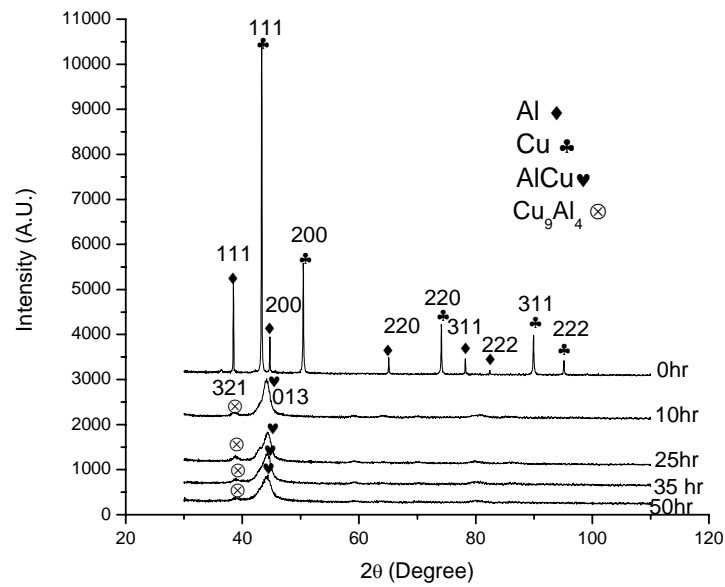
Fig 4.3 The XRD patterns of Al-Cu powder particles at different intervals of milling time.

4.1.1.2 Crystallite size and lattice strain measurement

The crystallite size can be investigated by analyzing the X-ray diffraction patterns. For this purpose, as received and milled powders were analyzed using X-ray diffraction (XRD) methods with CuKα radiation. The XRD peak broadening was used to measure the crystallite size and lattice strain. The Philips X'pert High Score software has been used here to calculate the crystallite size and lattice strain.

The decrease of the grain size and lattice strain to characterize the activation process has been determined from the X-ray diffraction patterns. Although the accumulation of lattice strain is a measure of defect formation, determining the defect structure was found to be more difficult. The crystallite size and the lattice strain of the powder measured from the XRD peak broadening is shown as a function of milling time in Fig 4.4 and Fig 4.5.
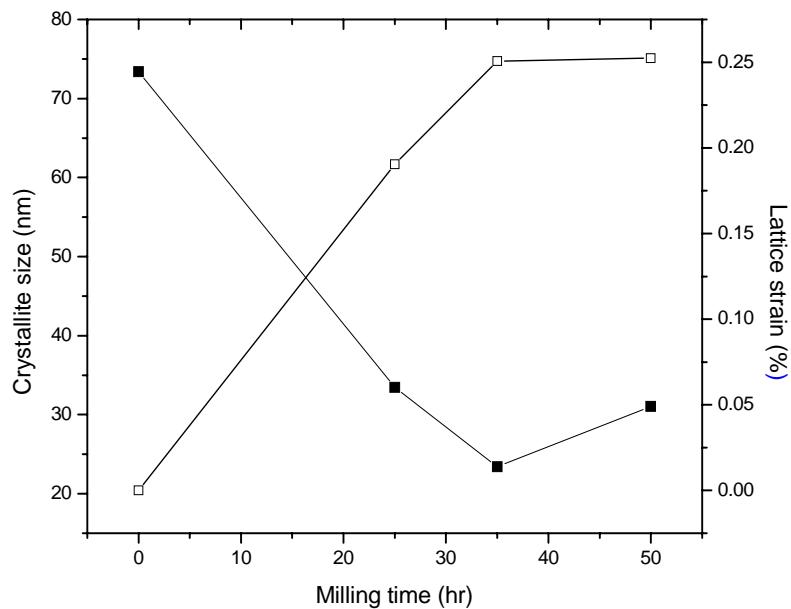
Fig 4.4 Crystallite size and lattice strain of the milled powder calculated from XRD patterns Vs milling time: Al.
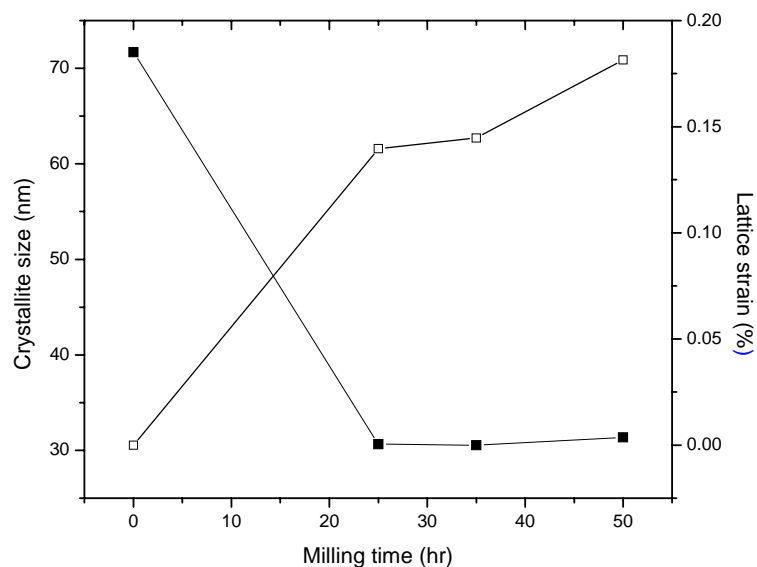
Fig 4.5 Crystallite size and lattice strain of the milled powder calculated from XRD patterns Vs milling time: Cu.

It can be seen that the crystallite size decreases and internal strain increases rapidly with milling time up to about 25 hours. With further milling the crystallite size remains almost constant, but the lattice strain appears to increase. In later stage of grinding, crystal size remains constant as equilibrium between cold welding and size reduction prevails. Whereas lattice strain increases continuously due to heavy plastic deformation between ball-powder-mill. It is found that the crystallite size has been reduced from 72 nm to 31nm for both Al and Cu, whereas lattice strain is increased from 0.1196 to 0.372% for Al and 0.1116 to 0.293% for Cu.

In case of Al-Cu powder, the crystallite size and the lattice strain of the powder measured from the XRD peak broadening is shown as a function of milling time in Table 4.1. It can be seen that the crystallite size decreases and internal strain increases with milling time. After 10 hours of milling, crystal size is around 21 nm which reduces to 6 nm after 50 hours of milling, whereas lattice strain is increased from 0.435 to 1.434 % for Al-Cu.

Table 4.1 Variation of crystallite size and lattice strain with milling time for Al-Cu alloy.

Milling time	Crystallite size (nm)	Lattice strain (%)
10 hr	21	0.435
25 hr	11	0.815
35 hr	9	1.028
50 hr	6	1.434

4.1.1.3 Particle size analysis

Particle size of the milled elemental metallic powder has been measured by nano particle size analyzer. Particle size of the milled powder has been shown in Fig 4.6. It is evident from the figure that particle size has been reduced from initial size 28 μm to 500 nm for Al and 28 μm to 400 nm for Cu. It is also clear from the figure that particle size distribution for Al is wide whereas for Cu it is narrow size distribution.
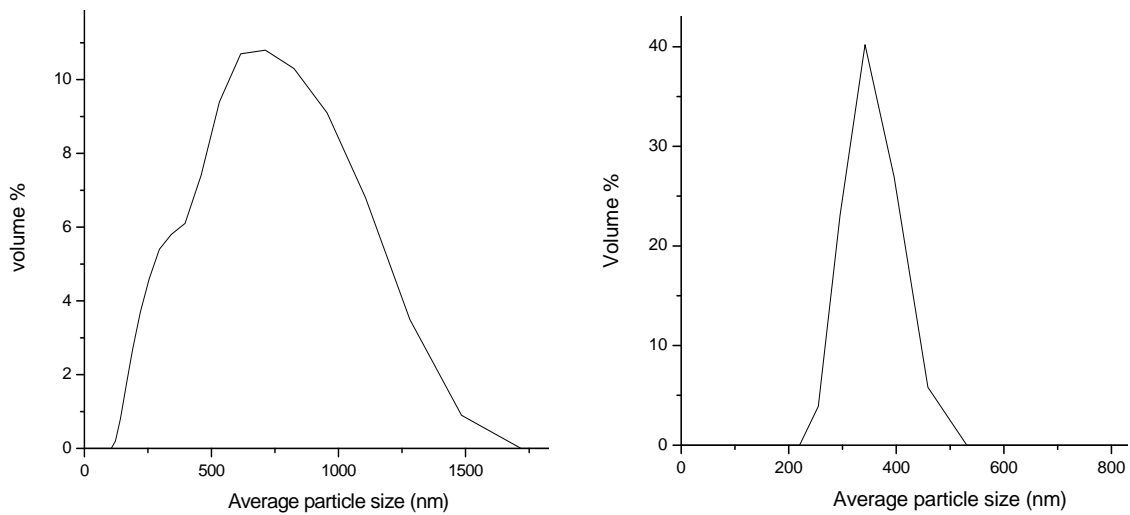
Fig 4.6 Particle size distribution of elemental metallic powders-deionized water-based nanofluids: Left (Al); Right (Cu).

In case of Al-Cu alloy, the particle size of alloy powder was measured by Malvern particle size analyzer. During the early stage of milling, the powder particles of Al and Cu (50 atomic weight %) were mixed together and then mechanically alloyed such that individual particles of Al and Cu could form nanocrystalline material. At a later stage, after about 10 h of milling,

the solid state reaction starts and considerable amounts of the product (Al-Cu) are formed. Fig 4.7 shows the particle size distribution of powder at different intervals of milling time. It is evident from the Fig 4.8 that average particle size has been reduced from initial size 21.0 μm to 3.0 μm. There was no evidence of welding, as particle size did not increase during the initial stages of milling. It should be mentioned that the size spectra corresponding to individually milled product of Al and Cu did not show any evidence of growth in particle size.
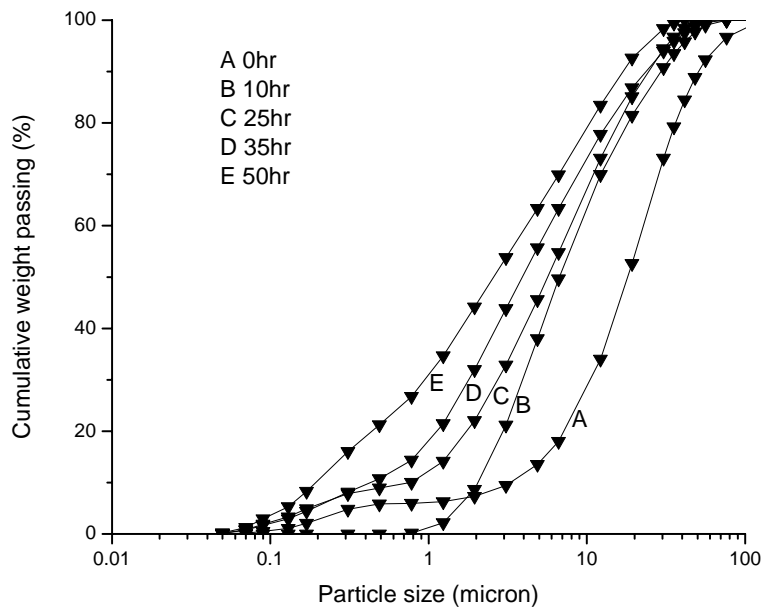
Fig 4.7 Particle size distribution of Al-Cu powder at different intervals of milling time.
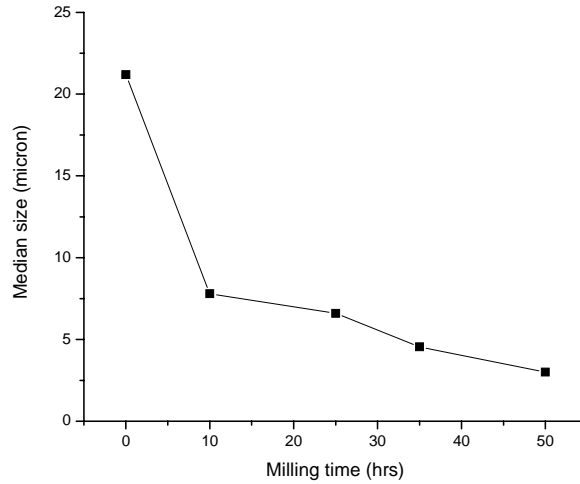
Fig 4.8 Variation of average Al-Cu particle size with milling time.

Particle size of the milled powder has also been measured by nano particle size analyzer. Particle size of the milled powder has been shown in Fig 4.9. It is evident from the figure that particle size has been reduced from initial size 28 μm to 500 nm for Al-Cu. Fig 4.9 shows that particle size distribution is a bi-modal kind of distribution which indicates that in one mode of distribution particles are observed up to around 1500 nm and in another mode of distribution size ranges from 3000-7000nm. The particle size distribution shows wide size distribution of particles.
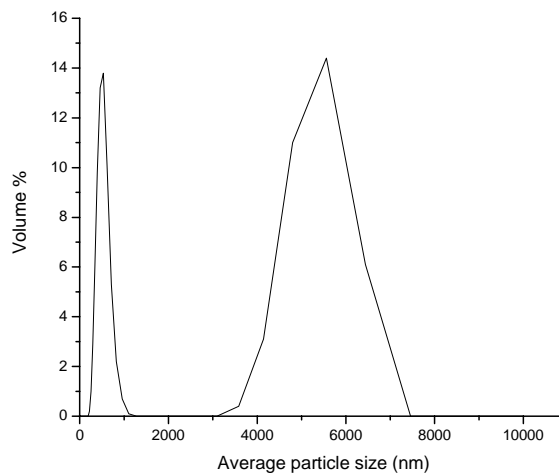

Fig 4.9 Particle size distribution of Al-Cu powder-deionized water-based nanofluids.

**4.1.1.4 Scanning electron microscopy (SEM) study**

The morphology and size of initial powders and also milled powders after different intervals of milling time were investigated with the help of scanning electron microscopy (SEM). The marker is set at 10 micron. Fig 4.10, Fig 4.11 and Fig 4.12 show the SEM micrographs of Al, Cu and Al-Cu alloy powder milled for different periods respectively. The micrographs show that powders of reacting materials are bulky with random shape and size at the initial stage of milling. The size of initial powders is around 28 μm. As the milling progresses the powders become more homogeneous. As regards particle size, it is also evident from the SEM images that it decreases gradually with increasing milling time. However, no evidence of particle coarsening could be obtained through SEM. The qualitative chemical analysis of Al-Cu powder milled for 50 hr was carried out using energy dispersive X-ray analysis. The EDS spectra show the peaks of Al and Cu along with C and O_2 as shown in Fig 4.13. O_2 comes from oxidation of powder during milling and C from steel balls and vials. The amount of O_2 and C is very small as X-ray diffraction can't detect the presence of these elements.
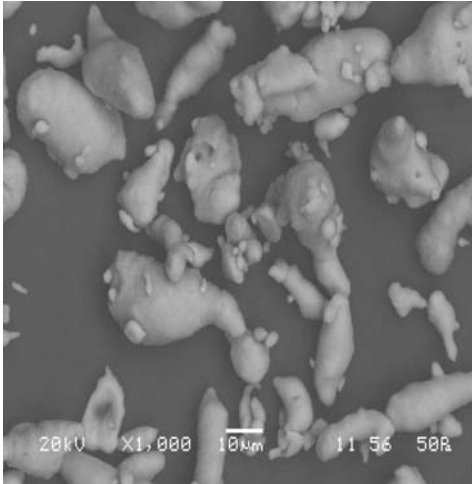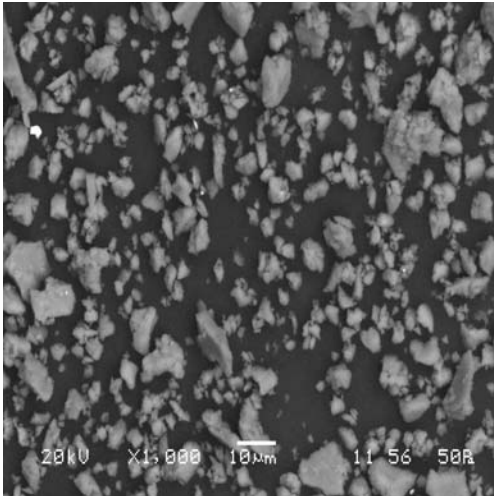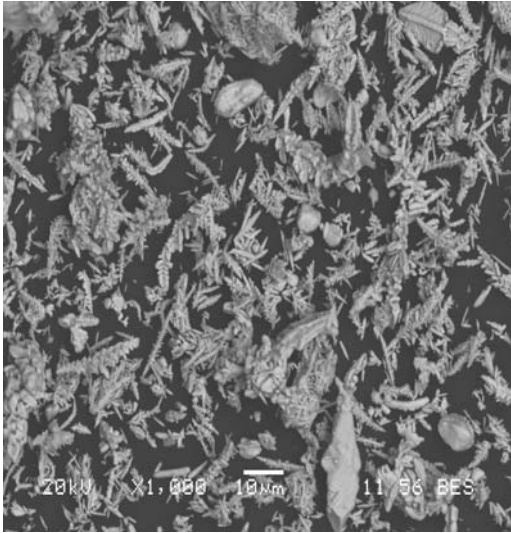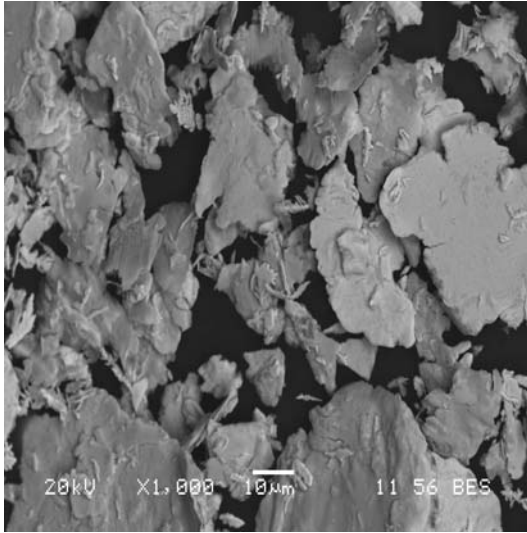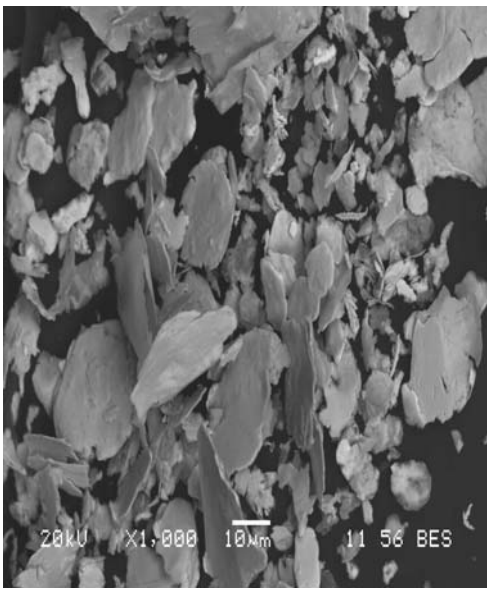
Al-0h
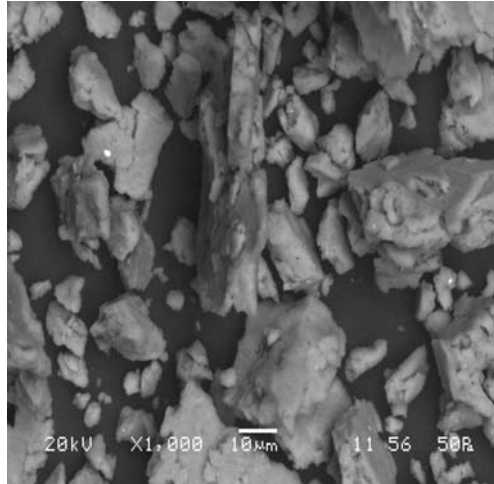
Al-25h
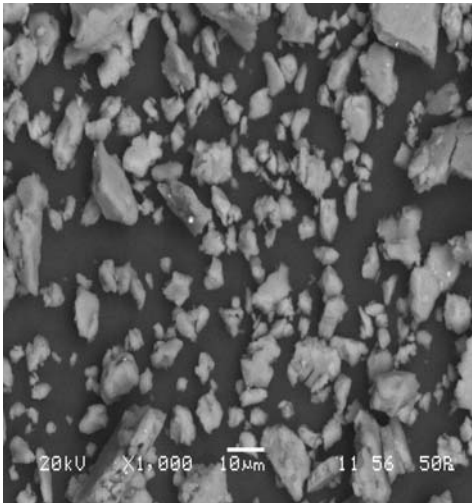
Al-35h

Al-50h

Fig 4.10 SEM micrographs of powder milled for different periods: Al.
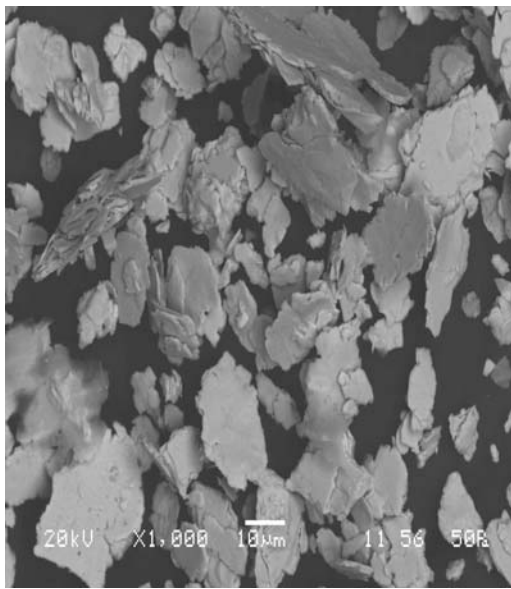
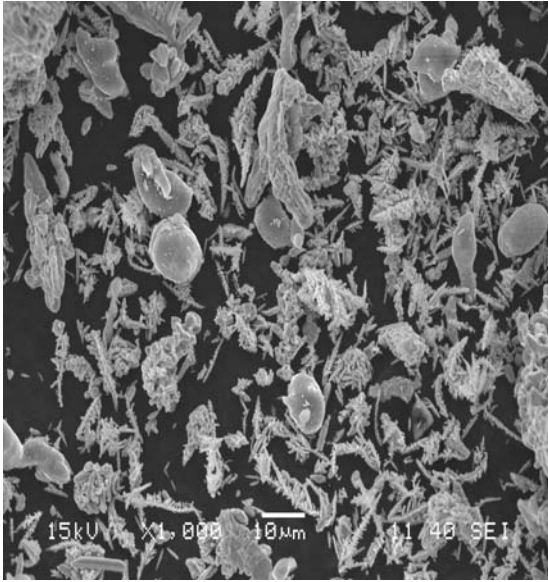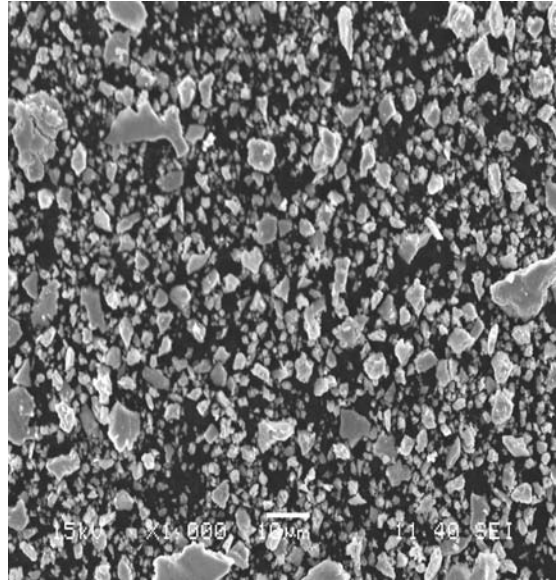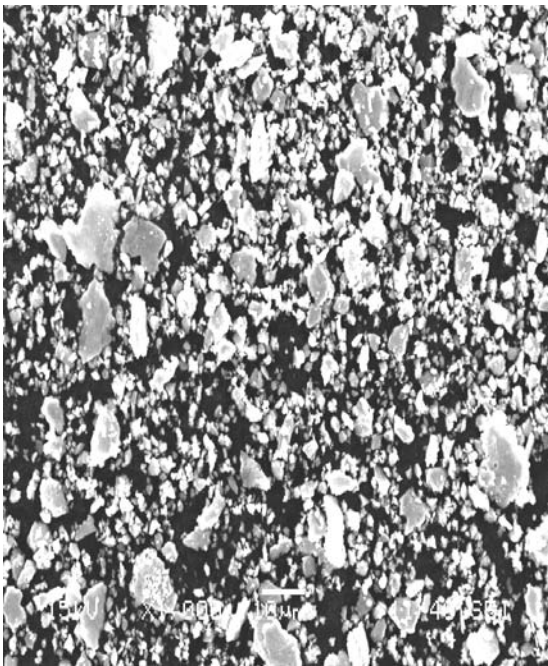|	
Cu-0h	Cu-10h

Cu-25h	Cu-50h

Fig 4.11 SEM micrographs of powder milled for different periods: Cu.
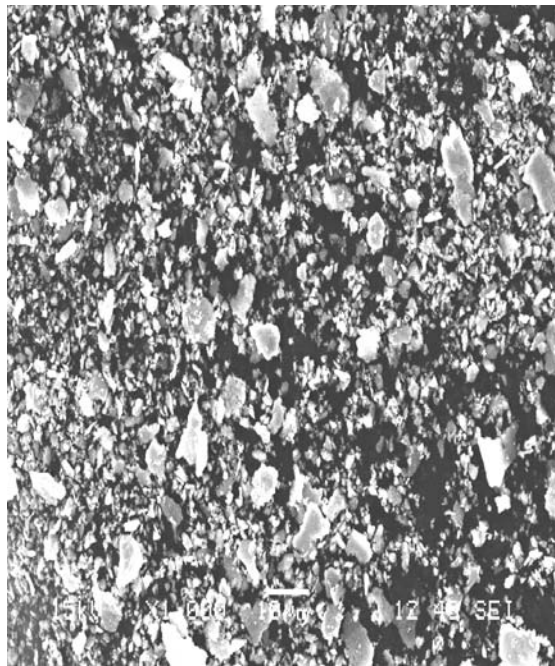
Al-Cu-0h

AlCu-25h

AlCu-35h

AlCu-50h

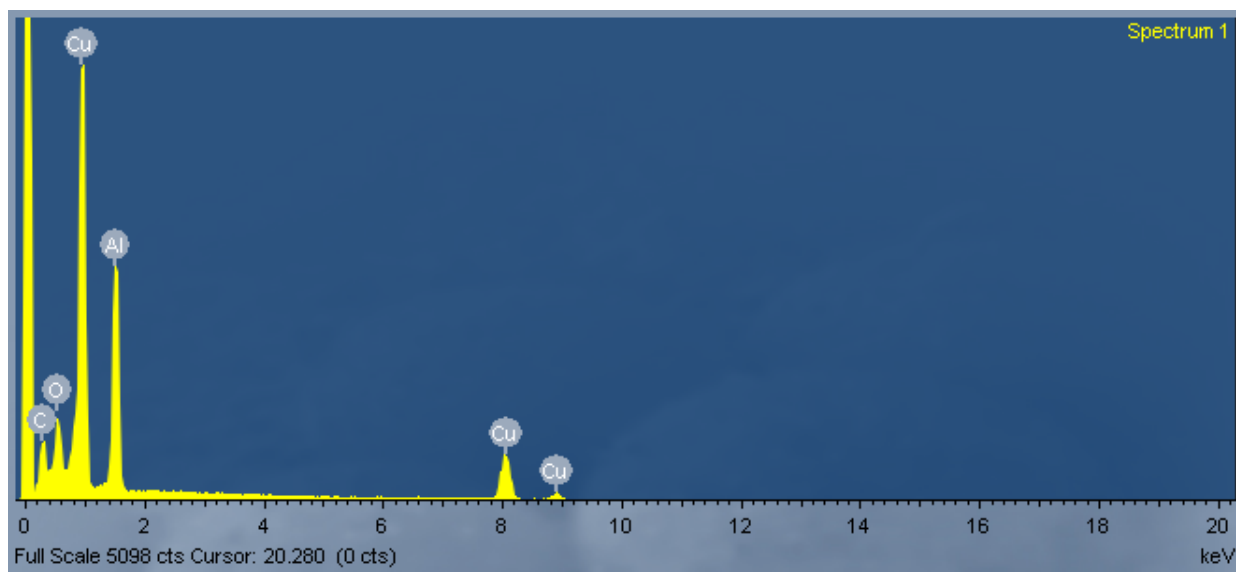Fig 4.12 SEM micrograph of different milled powder: Al-Cu.

Fig 4.13 EDX analysis of Al-Cu powder milled for 50 hr.

4.1.1.5 Transmission electron microscopy (TEM) study

The sample for TEM was prepared by adding a pinch of milled elemental metallic and alloy powder particles in the beaker containing acetone and kept in an ultrasonic bath for about 15 minute to get uniform dispersion of powder particles in the liquid. After that 2 drops of fluid containing dispersed particles were added in carbon coated Cu-grid and then dried. The desired sample was fixed in the sample holder of TEM for analyzing the internal structure of mechanically alloyed powder. Fig 4.14 shows the bright field TEM micrograph and corresponding SAD pattern of 50 hours milled powders. It is evident from the figure that the particle size is around 200-400 nm and contains large number of crystallites (size around 15-20 nm) with difference in contrast due to the variation of orientation. The SAD patterns for Al and Cu are sharp diffraction rings which indicate crystalline in nature, whereas the SAD pattern for Al-Cu alloy is slightly diffused hallow which indicates that powder particles are partial amorphous in nature.
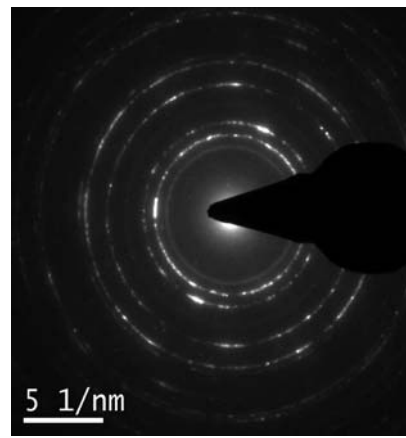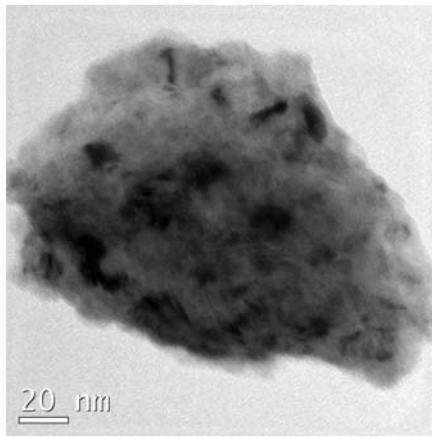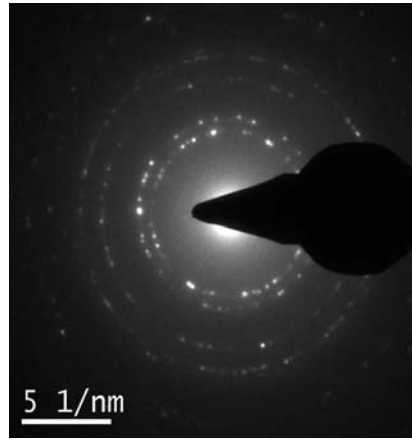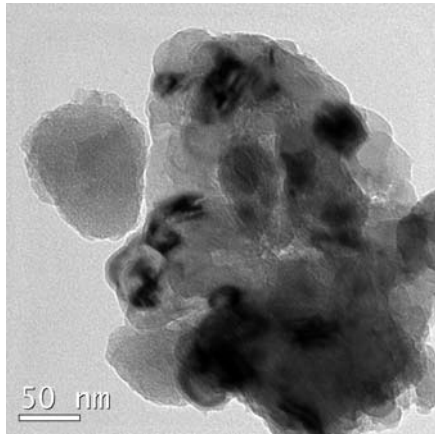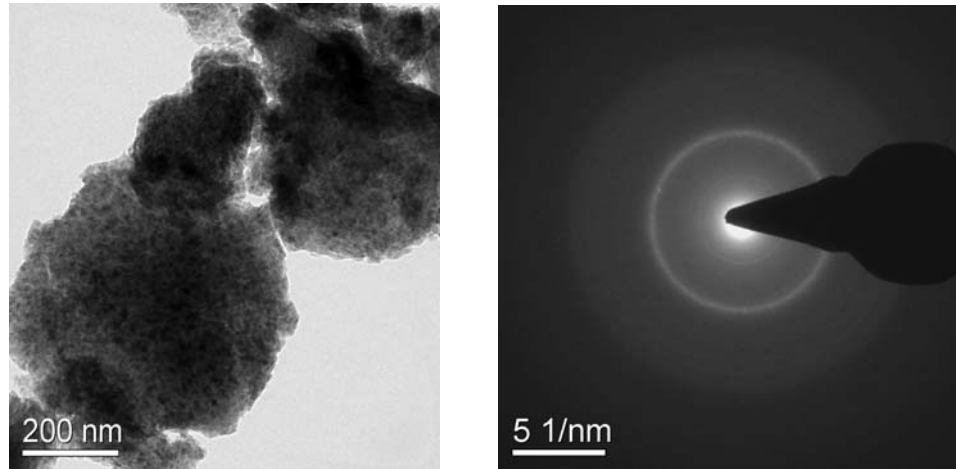
Fig 4.14 Bright Field TEM micrograph and corresponding SAD pattern: Al (Top), Cu (Middle) and Al-Cu (Bottom).

4.1.2 Dispersion stability of Al, Cu and Al-Cu ultrafine particles in nanofluid

The stability of Nanofluid was determined by measuring zeta potential values of elemental metallic and alloy powder dispersed in deionized water. However, for measurement of zeta potential, dilute fraction of metallic nano-suspension was selected here. The values of zeta potential ζ can be calculated by the Helmholtz-Smoluchowski equation.

$$\zeta = \mu^{\cup}\!\!\big/_{\varepsilon}$$

Where $\cup$ is the electrophoretic mobility, and μ, ε are the viscosity and the dielectric constant of the liquid in the boundary respectively.

In case of Cu powder particles, the zeta potential is zero at pH= 5.1, which is isoelectric point as shown in Fig 4.15. Therefore the force of electrostatic repulsion between particles is not sufficient to overcome the attraction force between particles and hence the dispersion is least stable. As pH increases or decreases by adding reacting reagent ammonium hydroxide (NH$_4$OH) or acetic acid respectively, then the particles tend to acquire more charge, so the electrostatic repulsion force between the particles becomes sufficient to prevent attraction and collision between particles caused by Brownian motion. Greater electrostatic force can also

lead to more free particles by increasing particle-particle distance so that the distance exceeds the hydrogen bonding range between particles and further reduces the probability of particle coagulation and settling and hence improving the dispersion stability of copper (Cu).

At pH = 2.3, the zeta potential becomes higher; the electrostatic repulsion force between particles is stronger, and the coagulated particles can redisperse through mechanical force. Therefore the dispersion stability of copper (Cu) is best at pH = 2.3 and corresponding zeta potential value is 14.6 mV. If pH-value is less than 2.3, then the zeta potential of particle surface and electrostatic repulsion force decreases due to compression of electrical double layer. Therefore, the suspension exhibits a poorer dispersion.

Similarly, for Al powder particles, the zeta potential is zero at pH = 8.9 which is isoelectric point as shown in Fig 4.15 and hence the dispersion is least stable. With decreasing pH value by adding reactant reagent, the stability tends to increase and therefore at pH = 2.5 the zeta potential becomes higher; the electrostatic repulsion force between particles is stronger, and the coagulated particles can redisperse through mechanical force. Therefore the dispersion stability of Al is best at pH=2.5 and corresponding zeta potential value is 54.63 mV. If pH-value is less than 2.5, then the zeta potential of particle surface and electrostatic repulsion force decreases due to compression of electrical double layer. Therefore, the suspension exhibits a poorer dispersion.
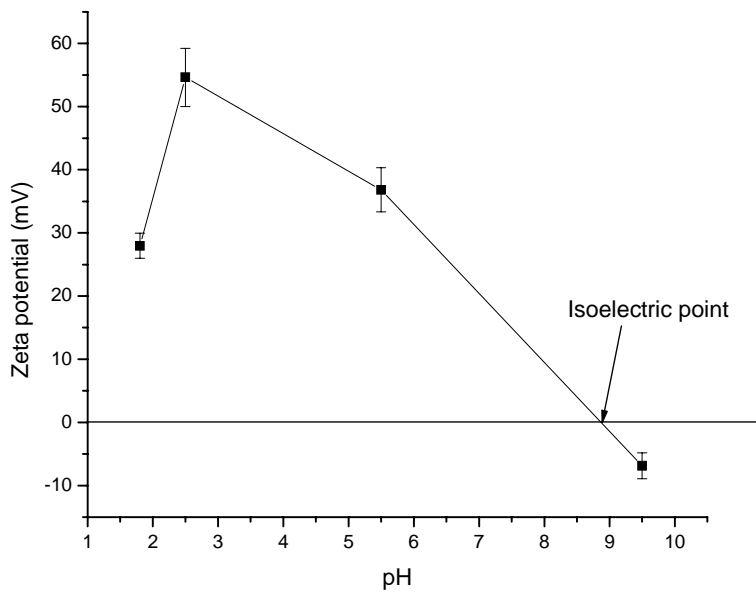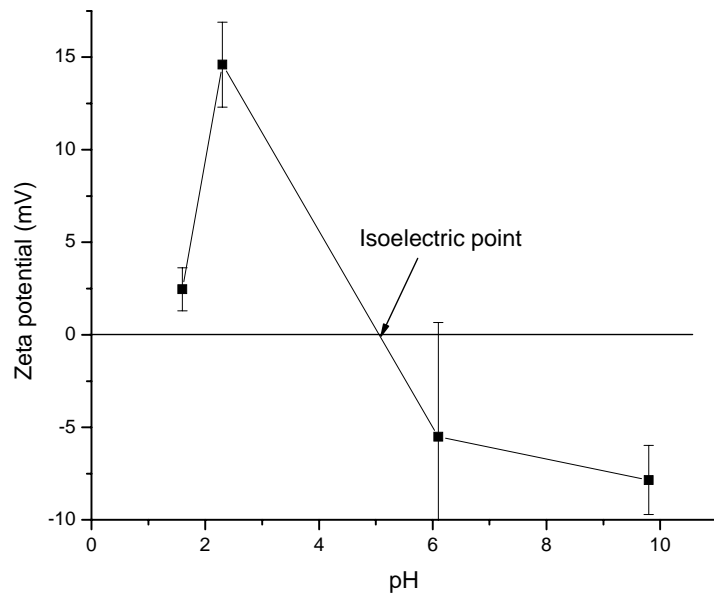
In case of Al-Cu alloy powder particles, the zeta potential is zero at pH= 9.7, which is isoelectric point as shown in Fig 4.15. Therefore the force of electrostatic repulsion between particles is not sufficient to overcome the attraction force between particles and hence the dispersion is least stable. At pH = 10.3 and 4.96, the zeta potential becomes higher; the electrostatic repulsion force between particles is stronger, and the coagulated particles can redisperse through mechanical force. Therefore the dispersion stability of Al-Cu alloy is best at pH=10.3 and 4.96 corresponding to zeta potential value of 49 and -27.7 mV. If pH-value is more than 10.3 or less than 4.96, then the zeta potential of particle surface and electrostatic repulsion force decreases due to compression of electrical double layer. Therefore, the suspension exhibits a poorer dispersion.

Fig 4.15 The evolution of zeta potentials of the deionized water-based elemental metallic and alloy powder nanofluids as a function of pH without surfactants. Top (Cu); Middle (Al) and Bottom (Al-Cu).

For Cu powder particles with the presence of surfactants, the zeta potential is zero at pH = 3.2 which is isoelectric point as shown in Fig 4.16. At pH = 9.8, the zeta potential becomes higher; the electrostatic repulsion force between particles is stronger, and the coagulated particles can redisperse through mechanical force. Therefore the dispersion stability of Cu is best at pH=9.8 corresponding to zeta potential value of -74.55 mV. If pH-value is more than 9.8, then the zeta potential of particle surface and electrostatic repulsion force decreases due to compression of electrical double layer. Therefore, the suspension exhibits a poorer dispersion.

Similarly, for Al powder particles with the presence of surfactants, the zeta potential is zero at pH = 3.3 which is isoelectric point as shown in Fig 4.16. At pH =5.5, the zeta potential becomes higher; the electrostatic repulsion force between particles is stronger, and the coagulated particles can redisperse through mechanical force. Therefore the dispersion stability of Al is best at pH=5.5 corresponding to zeta potential value of -55.5 mV. If pH-value is more than 5.5, then the zeta potential of particle surface and electrostatic repulsion

force decreases due to compression of electrical double layer. Therefore, the suspension exhibits a poorer dispersion.
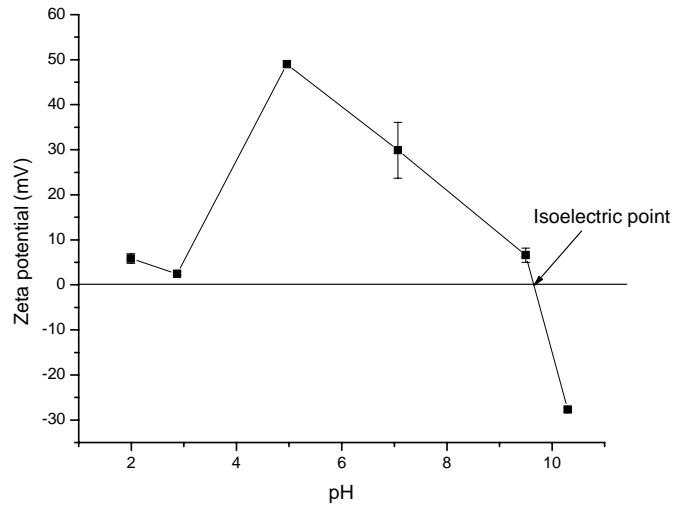
For Al-Cu alloy powder with the presence of surfactant, the zeta potential is zero at pH = 3.8 which is isoelectric point as shown in Fig 4.16. At pH = 9.5, the zeta potential becomes higher; the electrostatic repulsion force between particles is stronger, and the coagulated particles can redisperse through mechanical force. Therefore the dispersion stability of Al-Cu is best at pH=9.5 corresponding to zeta potential value of -90.6 mV. If pH-value is more than 9.5, then the zeta potential of particle surface and electrostatic repulsion force decreases due to compression of electrical double layer. Therefore, the suspension exhibits a poorer dispersion.
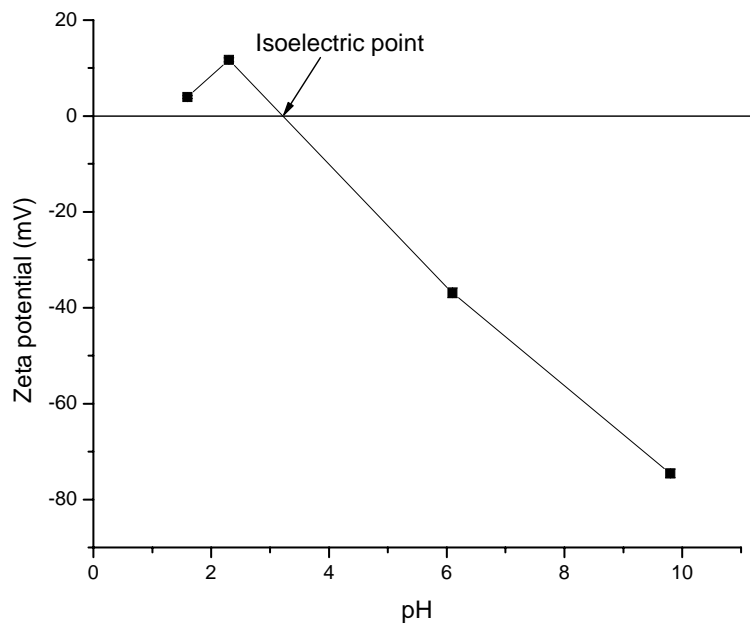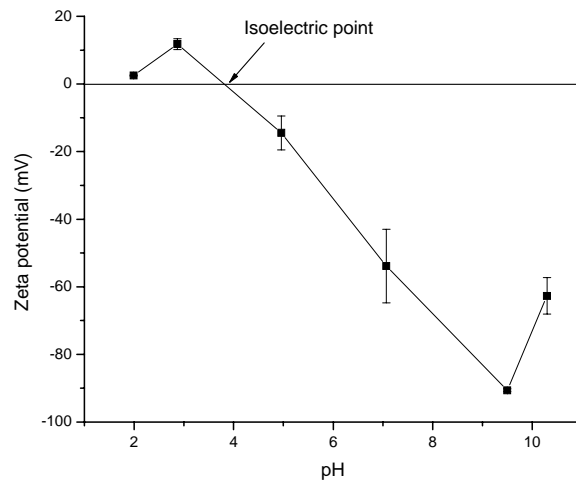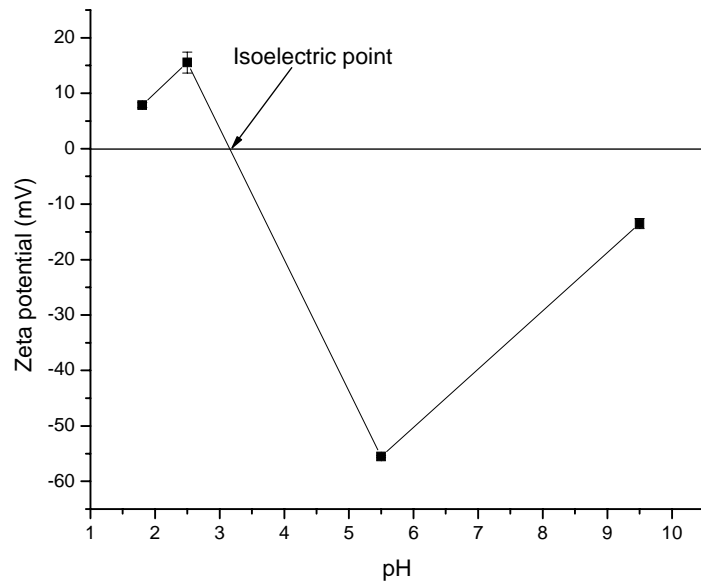
Fig 4.16 The evolution of zeta potentials of the deionized water-based elemental metallic and alloy powder nanofluids as a function of pH with surfactants. Top (Cu); Middle (Al) and Bottom (Al-Cu).

Fig 4.17 shows that the stabilization of Al-H_2O, Cu-H_2O, and Al-Cu-H_2O suspensions with the presence of oleic acid surfactant. Photographs indicate that ultrafine particles are

suspended in base fluid in the stationary state and no sediment is found, while the suspension without surfactant exhibits weaker dispersion and quickly occurs aggregatation.

Fig 4.17 Photographs of Al-H$_2$O (Left), Cu-H$_2$O (Middle), and Al-Cu-H$_2$O (Right) suspensions in presence of oleic acid surfactant.

4.2 Summary

Characterization of Al, Cu and Al-Cu ultrafine particles through X-ray diffraction (XRD) analysis, particle size analysis, scanning electron microscopy (SEM) study, and transmission electron microscopy (TEM) study is presented in this chapter. This chapter also provides the dispersion stability of ultrafine particles in base fluid.

Chapter – 5

Conclusions

5.1 Summary and conclusions

The following conclusions can be drawn from the present investigation:

1. It is possible to prepare ultrafine Al, Cu, and Al-Cu particles through mechanical alloying process by 50 hours of planetary ball milling.

2. The crystallite size decreases and internal strain increases rapidly with milling time up to about 25 hours. With further milling, the crystallite size remains almost constant but the lattice strain appears to increase. It is found from XRD that the crystallite size is around 31nm for both and lattice strain is 0.37%, 0.29 % for Al, Cu respectively.

3. In case of Al-Cu alloy, the alloy formation starts after 10 hours of milling. The crystallite size decreases and internal strain increases with milling time up to about 50 hours. It is found from XRD that the crystallite size is around 6 nm and lattice strain is 1.434 % for Al-Cu alloy.

4. The dispersion stability of Al and Cu ultrafine particles in base fluid is best at pH value of 2.5 and 2.3 corresponding to the zeta potential values of 54.63 and 14.60 mV without the presence of surfactants respectively. While in the presence of surfactant, the dispersion stability of Al and Cu nanoparticles in base fluid is best at pH value of 5.5 and 9.8 corresponding to the zeta potential values of -55.50 and -74.55 mV respectively.

5. Denser nanoparticles such as copper nanoparticles or those with a larger size tend to suspend at lower altitudes in coolants. However, nanoparticles with lower density such as Aluminum nanoparticles or those having a lower size tend to swim at higher altitudes within denser liquids such as aqueous solutions and liquid metals. Therefore, the dispersion stability of Al nanoparticles in nanofluids is better than that of Cu nanoparticles in nanofluids.

6. The dispersion stability of Al-Cu ultrafine particles in base fluid is best at pH value of 4.96, 10.3 corresponding to the zeta potential values of 49.00, -27.7 mV without the presence of surfactants respectively. While in the presence of surfactant, the dispersion stability of Al-Cu ultrafine particles in base fluid is best at pH value of 9.5 corresponding to the zeta potential value of -90.60 mV.

Chapter -6

Future Work

6.1 Future work

The present work leaves a wide scope for future investigators to explore many other aspects like study of thermal conductivity, viscosity and convective heat transfer of nanofluids. The electrokinetic phenomena of nanofluids like long term stability and particle interactions in the base fluids can also be studied.

Chapter -7

References

7.1 References

1. Maxwell, J.C., A Treatise on Electricity and Magnetism, 2nd ed., Oxford University Press, Cambridge, UK, 1904.

2. Choi, S.U.S., Enhancing Thermal Conductivity of Fluids with Nanoparticles: Developments and Applications of Non-Newtonian Flows, America Society of Mechanical Engineers (ASME) 66 (1995) pp. 99.

3. Feynman, Richard P., Lecture note "There's Plenty of Room at the Bottom" 29th December 1959 at the annual meeting of the American Physical Society at the California Institute of Technology (http://www.zyvex.com/nanotech/feynman.html).

4. Ryogo, K., J. Phys. Soc. Jpn., 17 (16) (1962) pp. 876–880.

5. Rohrer, H., The Nanoworld: Chances and Challenges, Microelectronic Engineering, 32 (1996) No. 1-4 pp. 5-14.

6. Sohn, L. L., A Quantum Leap for Electronics, Nature, 394 (1998) pp. 131-132.

7. Masuda, H., Ebata, A., Teramae, K., Hishiunma, K., Alternation of thermal conductivity and viscosity of liquid by dispersing ultrafine particles (dispersion of Al_2O_3, SiO_2 and TiO_2 ultrafine particles) Netsu Busei (Japan) 4 (1993) pp. 227-233.

8. Krishnamurthy, S., Bhattacharya, P., Phelan, P.E., Prasher, R.S., Enhanced mass transport in nanofluids, Nano Letter 6 (3) (2006) pp. 419–423.

9. Wasan, D.T., Nikolov, A.D., Spreading of nanofluids on solids, Nature 423 (2003) pp. 156–159.

10. Touloukian, Y. S., Powell, R. W., Ho, C. Y., and Klemens, P. G., Thermophysical Properties of Matter, Vol. 2, (1970) Plenum Press, New York.

11. Chopkar, M., Kumar, S., Bhandari, D.R., Das, P.K., Manna, I., Development and Characterization of Al_2Cu and Ag_2Al nanoparticles dispersed water and ethylene glycol based nanofluid, Material science and Engineering B 139 (2007) pp. 141-148.

12. Chopkar, M., Das, P.K., Manna, I., Synthesis and Characterization of nanofluid for advanced heat transfer applications, Scripta Materialia 55 (2006) pp. 549-552.

13. Lee, S., Choi, S.U.S., Li, S., and Eastman, J.A., Measuring thermal conductivity of fluids containing oxide nanoparticles, ASME Journal of Heat Transfer 121 (1999) pp. 280.

14. Eastman, J.A., Choi, S.U.S., Li, S., Yu, W., and Thompson, L.J., Anomalously increased effective thermal conductivity of ethylene glycol-based nanofluids containing copper nanoparticles, Applied Physics Letters 78 (2001) pp. 718–720.

15. Choi, S.U.S., Zhang, Z.G., Yu, W., Lockwood, F.E., and Grulke, E.A., Anomalous thermal conductivity enhancement in nanotube suspension, Applied Physics Letters 79 (2001) pp. 2252–2254.

16. Das, S.K., Putra, N., Thiesen, P., Roetzel, W., Temperature dependence of thermal conductivity enhancement for nanofluids, J. Heat Transfer 125 (2003) pp. 567–574.

17. Jana, S., Khojin, A.S., Zhong, W.H., Enhancement of fluid thermal conductivity by the addition of single and hybrid nano-additives, Thermochim. Acta 462 (2007) pp. 45–55.

18. Philip, J., Shima, P.D., Raj, B., Enhancement of thermal conductivity in magnetite based nanofluid due to chain like structure, Appl. Phys. Lett. 91 (2007) pp. 203108.

19. Zhou, D.W., Heat transfer enhancement of copper nanofluid with acoustic cavitation, Int. J. Heat Mass Transfer 47 (2004) pp. 3109–3117.

20. Hong, T.K., Yang, H.S., Choi, C.J., J. Appl. Phys. 97 (1999) pp. 280.

21. Xuan, Y., Li, Q., Heat transfer enhancement of nanofluids, International Journal of Heat and Fluid Flow 21 (2000) pp. 58–64.

22. Hamilton, R.L., Crosser, O.K., Thermal Conductivity of Heterogeneous Two Component Systems, Industrial and Engineering Chemistry Fundamentals 1 (1962) pp. 187–191.

23. Wang, X., Xu, X., Choi, S.U.S., Thermal conductivity of nanoparticles-fluid mixture, Journal of Thermophysics and Heat Transfer 13 (1999) pp. 474-480.

24. Keblinski, P., Phillpot, S.R., Choi, S.U.S., Eastman J.A., Mechanism of heat flow in suspensions of nanosized particles (nanofluids)International Journal of Heat and Mass Transfer 45 (2002) pp. 855–863.

25. Patel, H.E., Das, S.K., Sundararajan, T., Nair, A.S., George, B., Pradeep, T., Thermal conductivity of naked and monolayer protected metal nanoparticles based nanofluids: manifestation of anomalous enhancement and chemical effect, Applied Physics Letters 83 (2003) pp. 2931–2933.

26. Lee, D., Kim, J.W., Kim, B.G., A new parameter to control heat transport in nanofluids: surface charge state of the particle in suspension, Journal of Physical Chemistry B 110 (2006) pp. 4323–4328.

27. Murshed, S.M.S., Leong, K.C., Yang, C., Thermophysical and electrokinetic properties of nanofluids-A critical review, Applied Thermal Engineering 28 (2008) pp. 2109-2125.

28. Pak, B.C., Cho, Y.I., Hydrodynamic and heat transfer study of dispersed fluids with submicron metallic oxide particle, Experimental Heat Transfer 11 (1998) pp. 151–170.

29. Xuan, Y., Li, Q., Investigation of convective heat transfer and flow features of nanofluids, Journal of Heat Transfer-Transaction of ASME 125 (2003) pp. 151– 156.

30. Ding, Y., Alias, H., Wen, D., Williams, A.R., Heat transfer aqueous suspensions of carbon nanotubes (CNT nanofluids) International Journal of Heat and Mass Transfer 49 (2006) pp. 240-250.

31. Wen, D., Ding, Y., Experimental investigation into convective heat transfer of nanofluids at the entrance region under laminar flow conditions, International Journal of Heat and Mass Transfer 47 (2004) pp. 5181–5188.

32. Heris, S.Z., Etemad, S.G., Esfahany, M.S., Experimental investigation of oxide nanofluids laminar flow convective heat transfer, International Communications in Heat and Mass Transfer 33 (2006) pp. 529–535.

33. Lai, W.Y., Duculescu, B., Phelan, P.E., Prasher, R.S., Proceedings of ASME International Mechanical Engineering Congress and Exposition (IMECE 2006), Chicago, USA, 2006.

34. Jung, J.Y., Oh, H.S., Kwak, H.Y., Proceedings of ASME International Mechanical Engineering Congress and Exposition (IMECE 2006), Chicago, USA, 2006.

35. Choi, S.U.S., Nanofluid Technology: Current Status and Future Research, Energy Technology Division, Argonne National Laboratory, Argonne, IL. 60439.

36. Choi, S.U.S., Zhang, Z.G., Keblinski, P., Nanofluids, Encyclopedia of Nanoscience and Nanotechnology 6 (2004) pp. 757–773.

37. Zussman, S., New nanofluids increase heat transfer capability, Technology Transfer Highlights, vol. 8, Argonne National Laboratory, USA, 1997, pp. 4.

38. Choi, S.U.S., Xu, X., Keblinski, P., Yu, W., Nanofluids can take the heat, in: Proceedings of 20th Symposium on Energy Engineering Science, IL, USA, 2002.

39. Kim, P., Shi, L., Majumdar, A., Mc Euen, P.L., Thermal transport measurement individual multiwalled nanotubes, Phys. Rev. Lett. 87 (2001) pp. 215502.

40. Chaudhury, M.K., Complex fluids: spread the word about nanofluids, Nature, 423 (2003) pp. 131–132.

41. McQuiston, F.C., Parker, J.D., Spitler, J.D., Heating Ventilating and Air-Conditioning, John Wiley & Sons Inc., New York, 2000.

42. ASHRAE Handbook 1985 Fundamentals, American Society of Heating, Refrigerating and Air-Conditioning Engineers Inc., Atlanta, 1985.

43. Eastman, A., Choi, S.U.S., Li, S., Thompson, L.J., Proceedings of the Symposium on Nanophase and Nanocomposite Materials II, Materials Research Society, USA, vol. 457, (1997) pp. 3–11.

44. Tsung, T.T., Lo, CH., Jwo, C.S., Chang, H., Wang, K.C., A novel nanofluid manufacturing process using a cylindrical flow cooling method in an induction heating system, Int. J. Adv. Manuf. Technol., 29 (2006) pp. 99–104.

45. L., C.H., Tsung T.T., Chen, L.C., Shape-controlled synthesis of Cu-based nanofluid using submerged arc nanoparticles synthesis system (SANSS), J. Crys. Growth 277 (2005) pp. 636–642.

46. Chang, H., Chang, Y.C., Fabrication of Al_2O_3 nanofluid by a plasma arc nanoparticles synthesis system, J. Mater. Process Tech., 207 (2008) pp. 193–199.

47. Hwang, Y., Lee, J.K., Lee, J.K., Jeong, Y.M., Cheong, S.I., Ahn, Y.C., et al., Production and dispersion stability of nanoparticles in nanofluids, Powder Tech, 186 (2008) pp. 145–153.

48. Zhu, H.T., Li, Y.S, Yin, Y.S., A novel one-step chemical method for preparation of copper nanofluids. J. Colloid Interface Sci. 227 (2004) pp. 100–103.

49. Patungwasa, W., Hodak, J.H., pH tunable morphology of the gold nanoparticles produced by citrate reduction, Materials Chemistry & Physics 108 (2008) pp. 45–54.

50. Wu, J., and Liu, S., Low temperature growth of well-alligned ZnO nanorods by chemical vapor deposition, Adv. Mater. 14(3) (2002) pp. 215.

51. Gnanaprakash, G., Philip, J., Kumar, T.J., Raj, B., Effect of digestion time and alkali addition rate on the physical properties of magnetite nanoparticles, J. Phys. Chem. B 111 (2007) pp. 7978-7986.

52. Gnanaprakash, G., Philip, J., Raj, B., Effect of divalent metal hydroxide solubility product on the size of ferrite nanoparticles, Mater. Lett. 61 (2007) pp. 4545-4548.

53. Gnanaprakash, G., Mahadevan, S., Jayakumar, T., Kalyanasundaram, P., Philip, J., Raj, B., Effect of initial pH and temperature of iron salt solutions on formation of magnetite nanoparticles, Mater. Chem. Phys. 103 (2007) pp. 168-175.

54. Gnanaprakash, G., Ayyappan, S., Jayakumar, T., Philip, J., Raj, B., A simple method to produce magnetic nanoparticles with enhanced alpha to gamma-Fe_2O_3 phase transition temperature, Nanotechnology 17 (2006) pp. 5851-5857.

55. Bacri, J.C., Perzynski, R., Salin, D., Cabuil, V., Massart, R., Ionic magnetic fluids: a crossing of chemistry and physics, J. Magn. Magn. Mater. 85 (1990) pp. 27.

56. Kumar, R.V., Diamant, Y., Gedanken, A., Sonochemical synthesis and characterization of nanometer size transition metal oxides from metal acetates, Chem. Mater. 12 (2000) pp. 2301.

57. Okitsu, K., Yue, A., Tanabe, S., Matsumoto, H., Sonochemical preparation and catalytic bevaviour of highly dispersed palladium nanoparticles on alumina, Chem. Mater. 12 (2000) pp. 3006.

58. Carotenuto, G., Synthesis and characterization of poly (N-vinylpyrrolidone) filled by monodispersed silver clusters with controlled size, Appl. Organometal. Chem. 15 (2001) pp. 344.

59. Gurin, V.S., Alexeenko, A.A., Zolotovskaya, S.A., Yumashev, K.V., Copper and copper selenide nanoparticles in the solgel matrices: Structural and optical, Mater. Sci. Eng. C 26 (2006) pp. 952-955.

60. Li, S., Hui, Z., Yujie, J., Deren, Y., CuO nanodendrite synthesized by a novel hydrothermal route, Nanotechnology 15 (2004) pp. 1428.

61. Eftekhari, A., Molaei, F., Arami, H., Flower like bundles of ZnO nanosheets as an intermediate between hollow nanosphere and nanoparticles, Materials Science and Engineering A. 437 (2006) pp. 446-450.

62. Pastoriza-Santos, I., Liz-Marzan, L.M., Formation of PVP-protected metal nanoparticles in DMF, Langmuir 18 (2002) pp. 2888.

63. Yin, Y., Li, Z., Y., Zhong, Z., Gates, B., Xia, Y., N., Venkateswaran, S., Synthesis and characterization of stable aqueous dispersions of silver nanoparticles through the tollens process, J. Mater. Chem. 12 (2002) pp. 522.

64. Lin, X.Z., Teng, X., Yang, H., Direct synthesis of narrowly dispersed silver nanoparticles using a single-source precursor, Langmuir 19 (2003) pp. 10081.

65. Raveendran, P. , Fu, J., Wallen, S.L., Completely green synthesis and stabilization of metal nanoparticles, J. Am. Chem. Soc. 125 (2003) pp. 13940.

66. Zhu, J., Liu, S., Palchik, O., Koltypin, Y., Gedanken, A., Shape control synthesis of silver nanoparticles by pulse sonoelectrochemical methods, Langmuir 16 (2000) pp. 6396.

67. Penner, R.M., Mesoscopic metal particles and wires by electrodeposition, J. Phys. Chem. B 106 (2002) pp. 3339.

68. Yin, B., Ma, H., Wang, S., Chen, S., Electrochemical synthesis of silver nanoparticles under protection of poly (N-vinylpyrrolidone), J. Phys. Chem. B 107 (2003) pp. 8898.

69. Qiu, X.F., Xu, J.Z., Zhu, J.M., Zhu, J.J., Xu, S., Chen H.Y., Controllable synthesis of palladium nanoparticles via a simple sonoelectrochemical method, J. Mater. Res. 18 (2003) pp. 1399.

70. Bjerneld, E.J., Svedberg, F., Kall, M., Laser-induced growth and deposition of noble metal nanoparticles for surface enhanced Raman scattering, Nano Letters 3 (2003) pp. 593-596.

71. Fouchet, A., Prellier, W., Mercey, B., Mechin, L., Kulkarni, V. N. and Venkatesan, T., J. Investigation of laser ablated ZnO thin films grown with Zn metal target: a structural study, Appl. Phys. 96 (2004) pp. 3228.

72. Gleiter, H., Nanostructure materials: basic concepts and microstructure, Acta Mater. Rev.48 2000 1-29.

73. Suryanarayana, C., Nanocrystalline materials, Int.Mater.Rev.40 (2) (1995) pp. 41.

74. Gleiter, H., Nanocrystalline material, Progress in Material sci. 33 (1989) pp. 223-315.

75. Yujin, H., Lee, Jae-K., Lee, Jong-K., Jeong, Y.M., Cheong, S., Ahn, Y.C., Kim, Soo H., Production and dispersion stability of nanoparticles in nano fluids, Powder Technology, 186(2) (2008) pp. 145-153.

76. Kwak, K., Kim, C., Viscosity and thermal conductivity of copper oxide nanofluid dispersed in ethylene glycol, Korea-Australia Rheology Journal, 17 No. 2 (2005) pp. 35-40.